

Localization and universality of eigenvectors in directed random graphs

Fernando Lucas Metz

*Physics Institute, Federal University of Rio Grande do Sul, 91501-970 Porto Alegre, Brazil and
London Mathematical Laboratory, 18 Margravine Gardens, London W6 8RH, United Kingdom*

Izaak Neri

Department of Mathematics, King's College London, Strand, London, WC2R 2LS, UK

(Dated: April 4, 2024)

Although the spectral properties of random graphs have been a long-standing focus of network theory, the properties of right eigenvectors of directed graphs have so far eluded an exact analytic treatment. We present a general theory for the statistics of the right eigenvector components in directed random graphs with a prescribed degree distribution and with randomly weighted links. We obtain exact analytic expressions for the inverse participation ratio and show that right eigenvectors of directed random graphs with a small average degree are localized. Remarkably, if the fourth moment of the degree distribution is finite, then the critical mean degree of the localization transition is independent of the degree fluctuations, which is different from localization in undirected graphs that is governed by degree fluctuations. We also show that in the high connectivity limit the distribution of the right eigenvector components is solely determined by the degree fluctuations. For delocalized eigenvectors, we recover the universal results from standard random matrix theory that are independent of the degree distribution, while for localized eigenvectors the eigenvector distribution depends on the degree distribution.

Introduction. Complex systems, such as, neural networks [1–3], ecosystems [4], gene regulatory networks [5–7], social networks [8, 9], and the World Wide Web [10, 11] are described by large, directed graphs. Therefore, there is much interest in understanding how the topology of directed graphs impacts the dynamics of processes and algorithms on them.

Much insight in the dynamical processes on graphs is gained from the spectral properties of the adjacency matrix that represents the network. This is because the linearized dynamics of a complex system in the vicinity of a fixed point is determined by the spectral properties of the adjacency matrix [12, 13]. As a consequence, spectral analysis of the adjacency matrix has proven to be important in the study of neural networks [14–18], ecosystems [19–21], gene regulatory networks [22, 23], and disease spreading [24–28]. In these systems, the eigenvectors of the adjacency matrix determine the dynamical modes evoked by external perturbations. In addition, right eigenvectors of adjacency matrices of directed graphs are used in algorithms for node centrality [29–31], community detection [32–34], and matrix completion [35].

In disordered systems, eigenvectors localize when the strength of the disorder is large enough [36, 37]. Localized eigenvectors occupy a few vertices, whereas delocalized eigenvectors are extended over the whole system. The transition from a delocalized to a localized state leads to a qualitative change in the dynamics of processes and algorithms. For example, the localization transition implies a metal-insulator phase transition in solid state physics [36, 37], a transition from an algorithmic successful to a failure phase in spectral algorithms [31, 35, 38], and a transition from a regime where the linear dynamics of a large complex system is governed

by a finite number of vertices to a regime where the dynamics is governed by a finite fraction of all vertices. In the context of disease spreading, eigenvector localization implies that the fraction of infected vertices is very small right above the epidemic threshold [25].

For undirected random graphs, the localization of eigenvectors of the adjacency matrix has been well studied [25, 26, 36, 37, 39–49]. The eigenvector of the largest eigenvalue is localized if the maximal degree of the graph is larger than a certain value. Hence, degree fluctuations are crucial for the localization of eigenvectors in undirected graphs.

For directed random graphs, the statistical properties and the localization of eigenvectors have been studied for one-dimensional chains, such as, the Hatano-Nelson model [50–52] and its extensions to biological systems [53, 54], and a diluted Ginibre ensemble [55]. However, the localization of eigenvectors in directed random graphs that model complex systems, such as, the World Wide Web or neural networks, have not been studied so far.

In this Letter, we make a significant step forward by developing an exact theory for the statistical properties of the right (or left) eigenvectors of directed random graphs with a prescribed degree distribution and random couplings. We derive exact analytic expressions for the inverse participation ratio and for the critical point of the localization-delocalization transition. Surprisingly, when the moments of the degree distribution are finite, the critical point of the localization-delocalization transition is independent of the degree distribution. Moreover, the right eigenvectors are localized if the degree distribution has a diverging fourth moment. We also show that in the high connectivity limit the statistics of the components of right eigenvectors are only determined by degree

fluctuations. In this limit, we obtain distinct universality classes that depend on an exponent that quantifies the degree fluctuations.

Model set-up. We consider random matrices \mathbf{A} of dimension $n \times n$ with elements

$$A_{ij} = J_{ij} C_{ij}, \quad i, j \in \{1, 2, \dots, n\}, \quad (1)$$

where $C_{ij} \in \{0, 1\}$ are the entries of the adjacency matrix \mathbf{C} of a simple and directed random graph with a prescribed degree distribution

$$p_{K^{\text{in}}, K^{\text{out}}}(k, \ell) = p_{K^{\text{in}}}(k) p_{K^{\text{out}}}(\ell) \quad (2)$$

of indegrees K^{in} and outdegrees K^{out} . We set $C_{ij} = 1$ when there exists a directed link pointing from i to j , such that the outdegree (indegree) of the i -th node is $K_i^{\text{out}} = \sum_{j=1}^n C_{ij}$ ($K_i^{\text{in}} = \sum_{j=1}^n C_{ji}$). The J_{ij} are real-valued, independent and identically distributed random variables drawn from a distribution $p_J(x)$.

Random graph models with undirected edges and a prescribed degree distribution are surveyed in [56]. Here we consider their extension to the directed case. Directed random graphs with a prescribed degree distribution [57–62] model the World Wide Web [10, 11] and neural networks [1, 3, 63]. In this model, the indegrees and outdegrees are drawn from Eq. (2) subject to the constraint $\sum_{j=1}^n K_j^{\text{in}} = \sum_{j=1}^n K_j^{\text{out}}$, and subsequently nodes are randomly connected according to the given degree sequences. Hence, given a sequence of degrees, random graphs are drawn uniformly from the set of simple and directed graphs. This model provides the ideal setting to explore the influence of network topology on the spectral properties of \mathbf{A} .

In what follows, brackets $\langle \cdot \rangle$ denote the average with respect to the distribution of \mathbf{A} . In particular, we use

$$c = \langle K^{\text{out}} \rangle \quad (3)$$

for the mean outdegree, and we denote the variance of a random variable X by $\text{var}(X) = \langle X^2 \rangle - \langle X \rangle^2$.

Spectra of infinitely large matrices \mathbf{A} . The spectrum of \mathbf{A} has been studied in Refs. [64–67]. For $n \rightarrow \infty$ and $c > 1$, directed random graphs have a giant strongly connected component [68] and the spectral distribution $\rho_{\mathbf{A}}(\lambda) = n^{-1} \sum_{j=1}^n \delta(\lambda - \lambda_j(\mathbf{A}))$ of the eigenvalues $\{\lambda_j(\mathbf{A})\}_{j=1}^n$ is supported on a disk of radius $|\lambda_b| = \sqrt{c \langle J^2 \rangle}$ centered at the origin of the complex plane. In addition, if

$$c > c_{\text{gap}} = \frac{\langle J^2 \rangle}{\langle J \rangle^2}, \quad (4)$$

then there exists an eigenvalue outlier located at $\lambda_{\text{isol}} = c \langle J \rangle$ that is separated from the boundary λ_b by a finite gap. Figure 1 shows the eigenvalues for an example of a directed random graph, where one clearly identifies the outlier λ_{isol} and the boundary λ_b of $\rho_{\mathbf{A}}(\lambda)$ for $n \rightarrow \infty$.

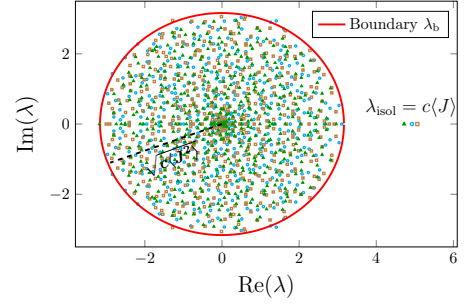


FIG. 1: Eigenvalues of three realizations (circles, triangles, and squares) of the adjacency matrix \mathbf{A} of directed random graphs with $n = 500$ (see Eq. (1)). The indegrees and outdegrees follow a Poisson distribution with average $c = 5$. The weights J_{ij} are drawn from a Gaussian distribution p_J with mean and variance equal to one.

Distribution of the right eigenvector components. A right eigenvector $\vec{R}(\lambda)$ associated to an eigenvalue λ of \mathbf{A} satisfies

$$\mathbf{A} \vec{R}(\lambda) = \lambda \vec{R}(\lambda), \quad (5)$$

and the distribution of the entries of $\vec{R}(\lambda)$ reads

$$p_R(r|\lambda) = \lim_{n \rightarrow \infty} \frac{1}{n} \sum_{i=1}^n \delta(r - R_i(\lambda)). \quad (6)$$

If λ is an outlier ($\lambda = \lambda_{\text{isol}}$) or λ is located at the boundary of the spectrum ($\lambda = \lambda_b$), then $p_R(r|\lambda)$ fulfills [65–67]

$$p_R(r|\lambda) = \sum_{k=0}^{\infty} p_{K^{\text{out}}}(k) \int \left(\prod_{j=1}^k dx_j d^2 r_j p_J(x_j) p_R(r_j|\lambda) \right) \times \delta \left(r - \frac{1}{\lambda} \sum_{j=1}^k x_j r_j \right), \quad (7)$$

where $d^2 r \equiv d \text{Re } r d \text{Im } r$. Equation (7) is exact for infinitely large and directed random graphs with a prescribed degree distribution, because they are locally tree-like. In fact, the solutions of Eq. (7) are well corroborated by direct diagonalizations of large adjacency matrices [65–67]. The analytic results presented below follow from Eq. (7).

Inverse participation ratio. The localization of $\vec{R}(\lambda)$ can be characterized in terms of the inverse participation ratio (IPR) [44, 69, 70]

$$\mathcal{I}(\lambda) \equiv \lim_{n \rightarrow \infty} \frac{n \sum_{i=1}^n |R_i(\lambda)|^4}{(\sum_{i=1}^n |R_i(\lambda)|^2)^2} = \frac{\langle |R(\lambda)|^4 \rangle}{\langle |R(\lambda)|^2 \rangle^2}, \quad (8)$$

where we have used that \mathcal{I} is self-averaging [71]. The IPR is finite if $\vec{R}(\lambda)$ is delocalized, whereas $\mathcal{I}(\lambda)$ diverges if $\vec{R}(\lambda)$ is localized on a finite number of nodes.

From Eq. (7), we derive in the Supplemental Material [71] exact expressions for the IPR when $\lambda = \lambda_{\text{isol}}$ or $\lambda = \lambda_b$. We find that

$$\mathcal{I}(\lambda_b) = \frac{(\gamma + 1) [\langle (K^{\text{out}})^2 \rangle - c]}{c(c - \langle J^4 \rangle / \langle J^2 \rangle^2)}, \quad (9)$$

where $\gamma = 2$ when $\lambda_b \in \mathbb{R}$ and $\gamma = 1$ when $\lambda_b \notin \mathbb{R}$. Analogously, the IPR at $\lambda = \lambda_{\text{isol}}$ reads

$$\begin{aligned} \mathcal{I}(\lambda_{\text{isol}}) = & \frac{3\beta_1 \langle J^2 \rangle^2}{(c^4 \langle J^4 \rangle - c \langle J^4 \rangle)} + \frac{\beta_3 (c^2 \langle J^2 \rangle^2 - c \langle J^2 \rangle)^2}{\beta_1^2 (c^4 \langle J^4 \rangle - c \langle J^4 \rangle)} \\ & + \frac{12\beta_1 \langle J^3 \rangle \langle J^2 \rangle (c^2 \langle J^2 \rangle^2 - c \langle J^2 \rangle)}{(c^4 \langle J^4 \rangle - c \langle J^4 \rangle) (c^3 \langle J^3 \rangle - c \langle J^3 \rangle)} \\ & + \frac{4\beta_2 \langle J^3 \rangle (c^2 \langle J^2 \rangle^2 - c \langle J^2 \rangle)^2}{\beta_1 (c^4 \langle J^4 \rangle - c \langle J^4 \rangle) (c^3 \langle J^3 \rangle - c \langle J^3 \rangle)} \\ & + \frac{6\beta_2 \langle J^2 \rangle (c^2 \langle J^2 \rangle^2 - c \langle J^2 \rangle)}{\beta_1 (c^4 \langle J^4 \rangle - c \langle J^4 \rangle)}, \end{aligned} \quad (10)$$

where

$$\beta_\ell \equiv \sum_{k=\ell+1}^{\infty} p_{K^{\text{out}}}(k) \frac{k!}{(k-\ell-1)!}, \quad \ell = 1, 2, 3. \quad (11)$$

Figure 2 illustrates Eqs. (9) and (10) as a function of c for a Gaussian distribution p_J and three different outdegree distributions: Poisson, exponential, and Borel distribution (see Supplemental Material [71]). All moments of these degree distributions are finite and each $p_{K^{\text{out}}}$ is parametrized only by c . Figure 2 shows that the IPR is finite if c is large enough and it diverges for small c , which demonstrates the existence of a delocalization-localization phase transition in directed random graphs.

The localization phase transition. There are two mechanisms for localization, one governed by fluctuations of J_{ij} , and a second one governed by degree fluctuations.

The first mechanism is illustrated in Fig. 2 and it holds for arbitrary $p_{K^{\text{out}}}$ with a finite fourth moment. In this case, the right eigenvectors associated to $\lambda = \lambda_b$ and $\lambda = \lambda_{\text{isol}}$ are localized when c is smaller than

$$c_b = \frac{\langle J^4 \rangle}{\langle J^2 \rangle^2} \quad \text{and} \quad c_{\text{isol}}^3 = \frac{\langle J^4 \rangle}{\langle J \rangle^4}, \quad (12)$$

respectively. Thus, the critical points for the localization transitions only depend on the lower moments of p_J and they are independent of $p_{K^{\text{out}}}$. When $p_J(x) = \delta(x-1)$, we obtain $c_b = c_{\text{isol}} = 1$ and the delocalization-localization transition is governed by the percolation transition for the strongly connected component [68]. According to Eq. (10), a localization transition at $c_{\text{isol}}^* = \sqrt{\langle J^3 \rangle / \langle J \rangle^3}$ is in principle possible, but we could not find an example of p_J for which $c_{\text{isol}}^* > c_{\text{isol}}$ and $c_{\text{isol}}^* > c_{\text{gap}}$.

Figure 3 shows the phase diagram when p_J is a Gaussian distribution with mean μ and variance σ^2 . In this case, c_{gap} , c_b and c_{isol} only depend on σ/μ . A few

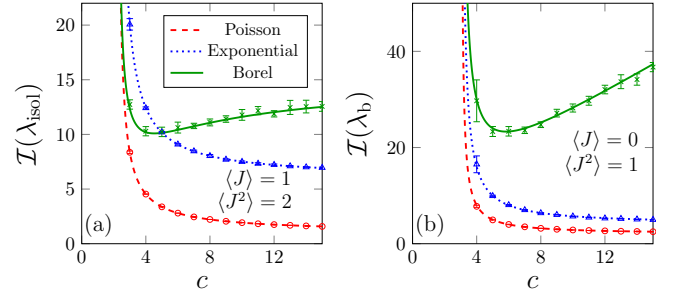


FIG. 2: The IPR $\mathcal{I}(\lambda)$ of right eigenvectors associated to λ_{isol} [Panel (a)] and $\lambda_b \notin \mathbb{R}$ [Panel (b)]. Equations (9) and (10) (different line styles) are shown as a function of the average degree c for different outdegree distributions: Poisson, exponential, and Borel (see Supplemental Material [71]). The weights J_{ij} are drawn from a Gaussian distribution p_J with first and second moments indicated on each panel. The symbols are obtained from the numerical solutions of Eq. (7) using the population dynamics algorithm [43, 66], while direct diagonalization results for $\mathcal{I}(\lambda)$ are presented in the Supplemental Material [71]. The error bars are the standard deviation of the IPR for 10 independent runs of population dynamics. The results for the Borel distribution are rescaled as $\mathcal{I}(\lambda_{\text{isol}}) \rightarrow \mathcal{I}(\lambda_{\text{isol}})/c$ in panel (a).

generic properties of eigenvector localization in directed random graphs, which also hold for non-Gaussian p_J , are illustrated in Fig. 3. First, $\vec{R}(\lambda_{\text{isol}})$ is delocalized when $\langle J^2 \rangle^3 > \langle J^4 \rangle \langle J \rangle^2$ because $c_{\text{gap}} > c_{\text{isol}}$. Second, the transition lines fulfill $c_{\text{gap}} < c_{\text{isol}} < c_b$ for $\langle J^2 \rangle^3 < \langle J^4 \rangle \langle J \rangle^2$. Lastly, the critical transitions c_{gap} , c_{isol} and c_{gap} intersect in a common point because $c_{\text{isol}}^3 = c_b c_{\text{gap}}^2$.

The second mechanism for localization is due to large degree fluctuations. From Eqs. (9) and (10), it follows that $\mathcal{I}(\lambda_b) \rightarrow \infty$ if $\langle (K^{\text{out}})^2 \rangle \rightarrow \infty$ and $\mathcal{I}(\lambda_{\text{isol}}) \rightarrow \infty$ if $\langle (K^{\text{out}})^4 \rangle \rightarrow \infty$, independently of p_J . Hence, localization of $\vec{R}(\lambda_b)$ and $\vec{R}(\lambda_{\text{isol}})$ also occurs in graphs with power-law degree distributions. In the sequel, we show that degree-based localization persists in the high connectivity limit.

Localization and universality in the high connectivity limit. In Fig. 2, $\mathcal{I}(\lambda)$ flows to different asymptotic values for $c \gg 1$. To explore the localization and universality of eigenvectors in the high connectivity limit $c \rightarrow \infty$, we analyze the moments of the distribution p_R . Since $\langle R(\lambda_{\text{isol}}) \rangle$ is finite, we characterize the limit $c \rightarrow \infty$ of $p_R(r|\lambda_{\text{isol}})$ through the relative variance

$$\mathcal{R}_c = \frac{\text{var}[R(\lambda_{\text{isol}})]}{\langle R(\lambda_{\text{isol}}) \rangle^2}. \quad (13)$$

On the other hand, since $\langle R(\lambda_b) \rangle = 0$, we characterize the limit $c \rightarrow \infty$ of $p_R(r|\lambda_b)$ through the kurtosis

$$\mathcal{K}_c = \frac{\langle (\text{Re } R(\lambda_b))^4 \rangle}{\langle (\text{Re } R(\lambda_b))^2 \rangle^2} = \frac{(4-\gamma)}{2} \mathcal{I}(\lambda_b), \quad (14)$$

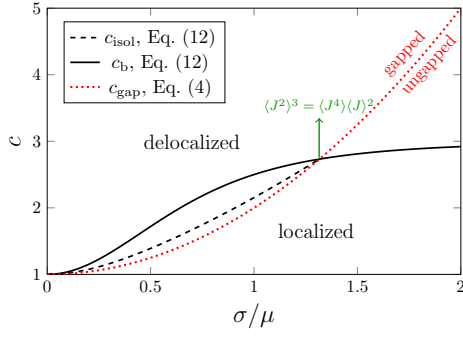


FIG. 3: Phase diagram for the localization of right eigenvectors associated to λ_{isol} and λ_b . The distribution p_J is Gaussian with mean μ and standard deviation σ .

where we used the fact that odd moments of $p_R(r|\lambda_b)$ are zero [71]. Setting $c \rightarrow \infty$ in Eqs. (13) and (14), we obtain [71]

$$\mathcal{R}_\infty = \lim_{c \rightarrow \infty} \frac{\text{var}[K^{\text{out}}]}{c^2}, \quad (15)$$

$$\mathcal{K}_\infty = 3 \left(1 + \lim_{c \rightarrow \infty} \frac{\text{var}[K^{\text{out}}]}{c^2} \right), \quad (16)$$

which indicates that the limit $c \rightarrow \infty$ of p_R is determined by the degree distribution. We see that, in general, $p_R(r|\lambda_b)$ and $p_R(r|\lambda_{\text{isol}})$ are not Gaussian in the high connectivity limit.

With the purpose of classifying the universal behavior of p_R for $c \rightarrow \infty$, let us consider degree distributions that satisfy

$$\text{var}[K^{\text{out}}] = Bc^\alpha \quad (c \gg 1), \quad (17)$$

where α and B depend on the specific choice of $p_{K^{\text{out}}}(k)$. Equation (17) holds for different examples of degree distributions, including those in Fig. 2. Plugging this *ansatz* for $\text{var}[K^{\text{out}}]$ in Eqs. (15) and (16), we obtain three universality classes for $\lim_{c \rightarrow \infty} p_R(r|\lambda)$, which are determined by the exponent α that controls the degree fluctuations. The results for the universality classes are summarized in table I. In terms of \mathcal{R}_∞ and \mathcal{K}_∞ , we find that for $\alpha \leq 2$ the eigenvectors $\vec{R}(\lambda_b)$ and $\vec{R}(\lambda_{\text{isol}})$ are delocalized in the limit $c \rightarrow \infty$, whereas for $\alpha > 2$ these eigenvectors are localized due to large degree fluctuations.

The eigenvector distributions in the high connectivity limit. The results in Table I indicate that $p_R(r|\lambda)$ is universal for $c \rightarrow \infty$. Below we present explicit expressions for $p_R(r|\lambda)$ when $c \rightarrow \infty$. Henceforth we set $\langle |R|^2 \rangle = 1$ without loosing generality.

The characteristic function of $p_R(r|\lambda)$ is given by [71]

$$g_R(u, v|\lambda) = \sum_{k=0}^{\infty} p_{K^{\text{out}}}(k) e^{k \ln F(u, v|\lambda)}, \quad (18)$$

	$\alpha < 2$	$\alpha = 2$	$\alpha > 2$
\mathcal{R}_∞	0	B	∞
\mathcal{K}_∞	3	$3(1+B)$	∞
Example	Poisson	Exponential	Borel

TABLE I: The relative variance \mathcal{R}_c of $\vec{R}(\lambda_{\text{isol}})$ and the kurtosis \mathcal{K}_c of $\vec{R}(\lambda_b)$ in the high connectivity limit $c \rightarrow \infty$ (see Eqs. (15) and (16)), together with an example of the out-degree distribution $p_{K^{\text{out}}}$ in each regime of α (see Eq. (17)).

where

$$F(u, v|\lambda) = \int dx p_J(x) \int d^2r p_R(r|\lambda) e^{-\frac{xzr}{2\lambda} + \frac{xz^*r^*}{2\lambda^*}}, \quad (19)$$

and $z = u + iv$. The symbol $(\dots)^*$ denotes complex-conjugation. If $\lambda \in \mathbb{R}$, the eigenvector components are real and $F(u, v|\lambda)$ is independent of v .

Setting $\lambda = \lambda_{\text{isol}}$ or $\lambda = \lambda_b$ in Eq. (19), we can expand $F(u, v|\lambda)$ for $c \gg 1$ up to order $O(1/c)$ if $\alpha \leq 2$ (see table I). This approach does not work for $\alpha > 2$, because the moments of p_R can diverge in this regime. Thus, performing this expansion for $\alpha \leq 2$ and substituting the resulting expression for $F(u, v|\lambda)$ in Eq. (18), we obtain [71]

$$g_R(u, v|\lambda_b) = \sum_{k=0}^{\infty} p_{K^{\text{out}}}(k) \exp \left[-\frac{\gamma k}{4c} (u^2 + (2 - \gamma)v^2) \right], \quad (20)$$

$$g_R(u, v|\lambda_{\text{isol}}) = \sum_{k=0}^{\infty} p_{K^{\text{out}}}(k) \exp \left(-\frac{iuk}{c\sqrt{Bc^{\alpha-2} + 1}} \right). \quad (21)$$

Remarkably, the characteristic functions for $c \rightarrow \infty$ are fully specified by $p_{K^{\text{out}}}$ and they are independent of p_J .

For degree distributions where $\lim_{c \rightarrow \infty} \text{var}[K^{\text{out}}]/c^2 = 0$ ($\alpha < 2$), it is reasonable to set $p_{K^{\text{out}}}(k) = \delta_{k,c}$ in Eqs. (20) and (21), leading to [71]

$$p_R(r|\lambda_b) = \frac{1}{\pi} e^{-|r|^2} \quad (\lambda_b \notin \mathbb{R}), \quad (22)$$

$$p_R(r|\lambda_{\text{isol}}) = \delta[\text{Im}(r)] \delta[\text{Re}(r) - 1]. \quad (23)$$

Equation (22) yields the well-known Porter-Thomas distribution for the eigenvector components of Gaussian random matrices [72, 73]. Thus, standard results from random matrix theory are recovered when $\alpha < 2$.

If $p_{K^{\text{out}}}$ is an exponential distribution, where $\alpha = 2$, we obtain in the limit $c \rightarrow \infty$ [71]

$$p_R(r|\lambda_b) = \frac{2}{\pi} K_0(2|r|) \quad (\lambda_b \notin \mathbb{R}), \quad (24)$$

$$p_R(r|\lambda_{\text{isol}}) = \sqrt{2} \delta[\text{Im}(r)] \Theta[\text{Re}(r)] e^{-\sqrt{2}\text{Re}(r)}, \quad (25)$$

where $\Theta(x)$ is the Heaviside step function and $K_0(x)$ is a modified Bessel function of the second kind [74]. Figure

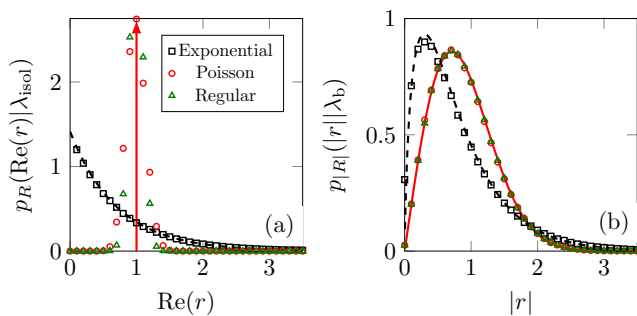


FIG. 4: The high connectivity limit $c \rightarrow \infty$ of the distribution $p_R(\text{Re}(r)|\lambda_{\text{iso}})$ of the real part of the eigenvector components at λ_{iso} [Panel (a)], and of the distribution $p_{|R|}(|r||\lambda_b)$ of the norm of the eigenvector components at $\lambda_b \notin \mathbb{R}$ [Panel (b)]. The solid red lines and the dashed black lines are, respectively, the analytic results for regular/Poisson and exponential degree distributions (see Eqs. (22-25)), while the symbols are numerical solutions of Eq. (7) with $c = 100$. The numerical data for regular/Poisson graphs in panel (a) is a Gaussian distribution with variance of $O(1/c)$, approaching the Dirac delta distribution (vertical arrow) for $c \rightarrow \infty$.

4 illustrates the shape of the distributions p_R given by Eqs. (22-25), and compares them with numerical solutions of Eq. (7) for $c = 100$. The derivation of Eqs. (22-25) is explained in the Supplemental Material [71].

Conclusions. We have shed light on the relationship between graph topology and the localization of right eigenvectors in directed random graphs. If the moments of the outdegree distribution $p_{K^{\text{out}}}$ are finite, then right eigenvectors at the edge of the spectrum are localized below a critical mean outdegree. It is striking that the critical points for the localization transitions are universal, in the sense they only depend on the lower moments of the distribution p_J of the edge weights, regardless of the network topology. Therefore, localization in directed random graphs is fundamentally different from localization in undirected graphs, for which degree fluctuations are important [25, 42–44, 46, 47, 75, 76]. Indeed, the eigenvector associated with the largest eigenvalue of the adjacency matrix of an undirected random graph is localized if the maximal degree is large enough [25]. Degree-based localization is also possible for directed random graphs, but then $p_{K^{\text{out}}}$ requires a divergent fourth moment.

In the high connectivity limit, the distribution p_R of the right eigenvector components is only determined by the graph topology, independently of p_J . If the outdegree fluctuations are small enough, then eigenvectors are delocalized and p_R is given by the same universal distribution as in the case of Gaussian random matrices [72, 73]. On the other hand, if the outdegree fluctuations are large enough, then eigenvectors are localized and the distribution p_R depends on $p_{K^{\text{out}}}$. More generally, these results indicate that Gaussian random matrix theory describes

well the spectral properties of high connectivity graphs only when the degree fluctuations are sufficiently small [77].

For future work, it would be interesting to explore the implications of eigenvector localization for the dynamics of neural networks [53, 54] and ecosystems [20, 78], to compare the theoretical predictions for the IPR with empirical values in real-world networks [26, 79], and to study eigenvector localization of Laplacians of directed graphs [80–82].

The authors thank Jacopo Grilli for interesting discussions. F.L.M. thanks London Mathematical Laboratory and CNPq/Brazil for financial support.

-
- [1] Nicolas Brunel, “Dynamics of sparsely connected networks of excitatory and inhibitory spiking neurons,” *Journal of computational neuroscience* **8**, 183–208 (2000).
 - [2] Ed Bullmore and Olaf Sporns, “Complex brain networks: graph theoretical analysis of structural and functional systems,” *Nature reviews neuroscience* **10**, 186–198 (2009).
 - [3] Olaf Sporns, *Networks of the Brain* (MIT press, 2010).
 - [4] Jordi Bascompte, “Disentangling the web of life,” *Science* **325**, 416–419 (2009).
 - [5] Ron Milo, Shai Shen-Orr, Shalev Itzkovitz, Nadav Kashtan, Dmitri Chklovskii, and Uri Alon, “Network motifs: simple building blocks of complex networks,” *Science* **298**, 824–827 (2002).
 - [6] Shai S Shen-Orr, Ron Milo, Shmoolik Mangan, and Uri Alon, “Network motifs in the transcriptional regulation network of *escherichia coli*,” *Nature genetics* **31**, 64–68 (2002).
 - [7] T I Lee and et al, “Transcriptional regulatory networks in *saccharomyces cerevisiae*,” *science* **298**, 799–804 (2002).
 - [8] Haewoon Kwak, Changhyun Lee, Hosung Park, and Sue Moon, “What is twitter, a social network or a news media?” in *Proceedings of the 19th international conference on World wide web* (2010) pp. 591–600.
 - [9] Luca Maria Aiello, Alain Barrat, Rossano Schifanella, Ciro Cattuto, Benjamin Markines, and Filippo Menczer, “Friendship prediction and homophily in social media,” *ACM Transactions on the Web (TWEB)* **6**, 1–33 (2012).
 - [10] Andrei Broder, Ravi Kumar, Farzin Maghoul, Prabhakar Raghavan, Sridhar Rajagopalan, Raymie Stata, Andrew Tomkins, and Janet Wiener, “Graph structure in the web,” *Computer networks* **33**, 309–320 (2000).
 - [11] Romualdo Pastor-Satorras and Alessandro Vespignani, *Evolution and structure of the Internet: A statistical physics approach* (Cambridge University Press, 2007).
 - [12] Philip Hartman, “A lemma in the theory of structural stability of differential equations,” *Proceedings of the American Mathematical Society* **11**, 610–620 (1960).
 - [13] David M Grobman, “Homeomorphism of systems of differential equations,” *Doklady Akademii Nauk SSSR* **128**, 880–881 (1959).
 - [14] Haim Sompolinsky, Andrea Crisanti, and Hans-Jurgen Sommers, “Chaos in random neural networks,” *Physical review letters* **61**, 259 (1988).
 - [15] Luis Carlos García Del Molino, Khashayar Pakdaman,

- Jonathan Touboul, and Gilles Wainrib, “Synchronization in random balanced networks,” *Physical Review E* **88**, 042824 (2013).
- [16] Jonathan Kadmon and Haim Sompolinsky, “Transition to chaos in random neuronal networks,” *Physical Review X* **5**, 041030 (2015).
- [17] Johnatan Aljadeff, Merav Stern, and Tatyana Sharpee, “Transition to chaos in random networks with cell-type-specific connectivity,” *Physical review letters* **114**, 088101 (2015).
- [18] Daniel Martí, Nicolas Brunel, and Srdjan Ostojic, “Correlations between synapses in pairs of neurons slow down dynamics in randomly connected neural networks,” *Physical Review E* **97**, 062314 (2018).
- [19] Robert M. May, “Will a large complex system be stable?” *Nature* **238**, 413–414 (1972).
- [20] Stefano Allesina, Jacopo Grilli, György Barabás, Si Tang, and Johnatan Aljadeff, “Predicting the stability of large structured food webs,” *Nat. Commun.* **6**, 7842 (2015).
- [21] Theo Gibbs, Jacopo Grilli, Tim Rogers, and Stefano Allesina, “Effect of population abundances on the stability of large random ecosystems,” *Physical Review E* **98**, 022410 (2018).
- [22] Yuxin Chen, Yang Shen, Pei Lin, Ding Tong, Yixin Zhao, Stefano Allesina, Xu Shen, and Chung-I Wu, “Gene regulatory network stabilized by pervasive weak repressions: microRNA functions revealed by the May–Wigner theory,” *National Science Review* **6**, 1176–1188 (2019), <https://academic.oup.com/nsr/article-pdf/6/6/1176/32351125/nwz076.pdf>.
- [23] Yipei Guo and Ariel Amir, “Stability of gene regulatory networks,” (2020), arXiv:2006.00018 [physics.bio-ph].
- [24] P. Van Mieghem, “Epidemic phase transition of the SIS type in networks,” *EPL (Europhysics Letters)* **97**, 48004 (2012).
- [25] A. V. Goltsev, S. N. Dorogovtsev, J. G. Oliveira, and J. F. F. Mendes, “Localization and spreading of diseases in complex networks,” *Phys. Rev. Lett.* **109**, 128702 (2012).
- [26] R. Pastor-Satorras and C. Castellano, “Eigenvector localization in real networks and its implications for epidemic spreading,” *J. Stat. Phys.* **173**, 1110–1123 (2018).
- [27] Cong Li, Huijuan Wang, and Piet Van Mieghem, “Epidemic threshold in directed networks,” *Phys. Rev. E* **88**, 062802 (2013).
- [28] Diogo H Silva and Silvio C Ferreira, “Dissecting localization phenomena of dynamical processes on networks,” arXiv preprint arXiv:2011.10918 (2020).
- [29] Phillip Bonacich, “Factoring and weighting approaches to status scores and clique identification,” *The Journal of Mathematical Sociology* **2**, 113–120 (1972), <https://doi.org/10.1080/0022250X.1972.9989806>.
- [30] Juan G. Restrepo, Edward Ott, and Brian R. Hunt, “Characterizing the dynamical importance of network nodes and links,” *Phys. Rev. Lett.* **97**, 094102 (2006).
- [31] Travis Martin, Xiao Zhang, and M. E. J. Newman, “Localization and centrality in networks,” *Phys. Rev. E* **90**, 052808 (2014).
- [32] Florent Krzakala, Cristopher Moore, Elchanan Mossel, Joe Neeman, Allan Sly, Lenka Zdeborová, and Pan Zhang, “Spectral redemption in clustering sparse networks,” *Proceedings of the National Academy of Sciences* **110**, 20935–20940 (2013).
- [33] Charles Bordenave, Marc Lelarge, and Laurent Massoulié, “Non-backtracking spectrum of random graphs: community detection and non-regular ramanujan graphs,” in *2015 IEEE 56th Annual Symposium on Foundations of Computer Science (IEEE, 2015)* pp. 1347–1357.
- [34] Tatsuro Kawamoto, “Algorithmic detectability threshold of the stochastic block model,” *Physical Review E* **97**, 032301 (2018).
- [35] Charles Bordenave, Simon Coste, and Raj Rao Nadakuditi, “Detection thresholds in very sparse matrix completion,” arXiv preprint arXiv:2005.06062 (2020).
- [36] Ragi Abou-Chacra, DJ Thouless, and PW Anderson, “A selfconsistent theory of localization,” *Journal of Physics C: Solid State Physics* **6**, 1734 (1973).
- [37] Michael Aizenman and Simone Warzel, “Extended states in a lifshitz tail regime for random schrödinger operators on trees,” *Physical review letters* **106**, 136804 (2011).
- [38] Olivier Giraud, Bertrand Georgeot, and Dima L. Shepelyansky, “Delocalization transition for the google matrix,” *Phys. Rev. E* **80**, 026107 (2009).
- [39] Yan V. Fyodorov and Alexander D. Mirlin, “Localization in ensemble of sparse random matrices,” *Phys. Rev. Lett.* **67**, 2049–2052 (1991).
- [40] Alexander D Mirlin and Yan V Fyodorov, “Localization transition in the anderson model on the bethe lattice: spontaneous symmetry breaking and correlation functions,” *Nuclear Physics B* **366**, 507–532 (1991).
- [41] SN Evangelou, “A numerical study of sparse random matrices,” *Journal of statistical physics* **69**, 361–383 (1992).
- [42] Michel Bauer and Olivier Golinelli, “Random incidence matrices: moments of the spectral density,” *Journal of Statistical Physics* **103**, 301–337 (2001).
- [43] Reimer Kühn, “Spectra of sparse random matrices,” *Journal of Physics A: Mathematical and Theoretical* **41**, 295002 (2008).
- [44] Fernando Lucas Metz, Izaak Neri, and Désiré Bollé, “Localization transition in symmetric random matrices,” *Physical Review E* **82**, 031135 (2010).
- [45] Yoshiyuki Kabashima and Hisanao Takahashi, “First eigenvalue/eigenvector in sparse random symmetric matrices: influences of degree fluctuation,” *Journal of Physics A: Mathematical and Theoretical* **45**, 325001 (2012).
- [46] F. Slanina, “Localization of eigenvectors in random graphs,” *Eur. Phys. J. B* **85**, 361 (2012).
- [47] R. Pastor-Satorras and C. Castellano, “Distinct types of eigenvector localization in networks,” *Sci. Rep.* **6**, 18847 (2016).
- [48] KS Tikhonov, AD Mirlin, and MA Skvortsov, “Anderson localization and ergodicity on random regular graphs,” *Physical Review B* **94**, 220203 (2016).
- [49] Vito A R Susca, Pierpaolo Vivo, and Reimer Kühn, “Top eigenpair statistics for weighted sparse graphs,” *Journal of Physics A: Mathematical and Theoretical* **52**, 485002 (2019).
- [50] Naomichi Hatano and David R Nelson, “Localization transitions in non-hermitian quantum mechanics,” *Physical review letters* **77**, 570 (1996).
- [51] Naomichi Hatano and David R Nelson, “Vortex pinning and non-hermitian quantum mechanics,” *Physical Review B* **56**, 8651 (1997).
- [52] Joshua Feinberg and A Zee, “Non-hermitian localization and delocalization,” *Physical Review E* **59**, 6433 (1999).
- [53] Ariel Amir, Naomichi Hatano, and David R. Nel-

- son, “Non-hermitian localization in biological networks,” *Phys. Rev. E* **93**, 042310 (2016).
- [54] Grace H. Zhang and David R. Nelson, “Eigenvalue repulsion and eigenvector localization in sparse non-hermitian random matrices,” *Phys. Rev. E* **100**, 052315 (2019).
- [55] Thomas Peron, Bruno Messias F. de Resende, Francisco A. Rodrigues, Luciano da F. Costa, and J. A. Méndez-Bermúdez, “Spacing ratio characterization of the spectra of directed random networks,” *Phys. Rev. E* **102**, 062305 (2020).
- [56] Bailey K. Fosdick, Daniel B. Larremore, Joel Nishimura, and Johan Ugander, “Configuring random graph models with fixed degree sequences,” *SIAM Review* **60**, 315–355 (2018), <https://doi.org/10.1137/16M1087175>.
- [57] Michael Molloy and Bruce Reed, “A critical point for random graphs with a given degree sequence,” *Random Structures & Algorithms* **6**, 161–180 (1995), <https://onlinelibrary.wiley.com/doi/pdf/10.1002/rsa.3240060200>.
- [58] M Molloy and B Reed, “The size of the giant component of a random graph with a given degree sequence,” *Combinatorics, Probability and Computing* **7**, 295–305 (1998).
- [59] Béla Bollobás and Bollobás Béla, *Random graphs*, 73 (Cambridge university press, 2001).
- [60] M. E. J. Newman, S. H. Strogatz, and D. J. Watts, “Random graphs with arbitrary degree distributions and their applications,” *Phys. Rev. E* **64**, 026118 (2001).
- [61] M. Newman, *Networks: An Introduction* (OUP Oxford, 2010).
- [62] Sergei N Dorogovtsev and José FF Mendes, *Evolution of networks: From biological nets to the Internet and WWW* (OUP Oxford, 2013).
- [63] Michael A Arbib, ed., *The handbook of brain theory and neural networks* (MIT press, 2003).
- [64] Tim Rogers and Isaac Pérez Castillo, “Cavity approach to the spectral density of non-hermitian sparse matrices,” *Phys. Rev. E* **79**, 012101 (2009).
- [65] Izaak Neri and Fernando Lucas Metz, “Eigenvalue outliers of non-hermitian random matrices with a local tree structure,” *Phys. Rev. Lett.* **117**, 224101 (2016).
- [66] Fernando Lucas Metz, Izaak Neri, and Tim Rogers, “Spectral theory of sparse non-hermitian random matrices,” *Journal of Physics A: Mathematical and Theoretical* **52**, 434003 (2019).
- [67] Izaak Neri and Fernando Lucas Metz, “Linear stability analysis of large dynamical systems on random directed graphs,” *Phys. Rev. Research* **2**, 033313 (2020).
- [68] S. N. Dorogovtsev, J. F. F. Mendes, and A. N. Samukhin, “Giant strongly connected component of directed networks,” *Phys. Rev. E* **64**, 025101 (2001).
- [69] Y V Fyodorov and A D Mirlin, “Statistical properties of eigenfunctions of random quasi 1d one-particle hamiltonians,” *Int. J. Mod. Phys. B* **8**, 3795–3842 (1994).
- [70] Konstantin Efetov, *Supersymmetry in disorder and chaos* (Cambridge University Press, 1999).
- [71] F. L. Metz and I. Neri, “see the supplemental material,” See Supplemental Material (2020).
- [72] C. E. Porter and R. G. Thomas, “Fluctuations of nuclear reaction widths,” *Phys. Rev.* **104**, 483–491 (1956).
- [73] Alexander D. Mirlin, “Statistics of energy levels and eigenfunctions in disordered systems,” *Physics Reports* **326**, 259 – 382 (2000).
- [74] I.S. Gradshteyn and I.M. Ryzhik, *Table of Integrals, Series, and Products* (Elsevier Science, 2014).
- [75] Michael Krivelevich and Benny Sudakov, “The largest eigenvalue of sparse random graphs,” *Combinatorics, Probability and Computing* **12**, 61–72 (2003).
- [76] Raj Rao Nadakuditi and M. E. J. Newman, “Spectra of random graphs with arbitrary expected degrees,” *Phys. Rev. E* **87**, 012803 (2013).
- [77] Fernando L. Metz and Jeferson D. Silva, “Spectral density of dense random networks and the breakdown of the wigner semicircle law,” *Phys. Rev. Research* **2**, 043116 (2020).
- [78] Jacopo Grilli, Tim Rogers, and Stefano Allesina, “Modularity and stability in ecological communities,” *Nat. Commun.* **7**, 12031 (2016).
- [79] Sergey N Dorogovtsev, Alexander V Goltsev, José FF Mendes, and Alexander N Samukhin, “Spectra of complex networks,” *Physical Review E* **68**, 046109 (2003).
- [80] J Ståring, B Mehlig, Yan V Fyodorov, and JM Luck, “Random symmetric matrices with a constraint: The spectral density of random impedance networks,” *Physical Review E* **67**, 047101 (2003).
- [81] AN Samukhin, SN Dorogovtsev, and JFF Mendes, “Laplacian spectra of, and random walks on, complex networks: Are scale-free architectures really important?” *Physical Review E* **77**, 036115 (2008).
- [82] Reimer Kühn, “Spectra of random stochastic matrices and relaxation in complex systems,” *EPL (Europhysics Letters)* **109**, 60003 (2015).
- [83] P. van Mieghem, *Graph Spectra for Complex Networks* (Cambridge University Press, 2012).
- [84] E. Borel, *C. R. Acad. Sci.* **214**, 452 (1942).
- [85] J. C. Tanner, “A derivation of the Borel distribution,” *Biometrika* **48**, 222–224 (1961), <https://academic.oup.com/biomet/article-pdf/48/1-2/222/607732/48-1-2-222.pdf>.

Supplemental material for “Localization and universality of eigenvectors in directed random graphs”

Fernando Lucas Metz

*Physics Institute, Federal University of Rio Grande do Sul, 91501-970 Porto Alegre, Brazil and
London Mathematical Laboratory, 18 Margravine Gardens, London W6 8RH, United Kingdom*

Izaak Neri

Department of Mathematics, Kings College London, Strand, London, WC2R 2LS, UK

(Dated: December 7, 2020)

S1. INTRODUCTION

The supplements are organized into four sections. In Sec. S2, we discuss the degree distributions we consider in the paper: regular, Poisson, exponential and Borel distributions. In Sec. S3, we derive Eqs. (9) and (10) in the main text for the inverse participation ratios $\mathcal{I}(\lambda_b)$ and $\mathcal{I}(\lambda_{\text{isol}})$, respectively. In Sec. S4, we derive the analytic results for the distribution of the eigenvector components in the high connectivity limit. Lastly, in Sec. S5, we compare theoretical results for the inverse participation ratio of infinitely large matrices with numerical results for matrices of finite size.

S2. DIRECTED RANDOM GRAPHS WITH A PRESCRIBED DEGREE DISTRIBUTION

In the present paper, we consider random graphs with a prescribed degree distribution

$$p_{K^{\text{in}}, K^{\text{out}}}(k, \ell) = p_{K^{\text{in}}}(k)p_{K^{\text{out}}}(\ell) \quad (\text{S1})$$

of indegrees K^{in} and outdegrees K^{out} , see Refs. [1–5]. Random graph models, in which the degree sequences are specified at the outset, are also called configuration models [1, 6]. We derive results for the spectral properties of simple graphs where self-edges and multi-edges are absent. A simple, weighted, and directed random graph instance, with degrees from a prescribed degree distribution $p_{K^{\text{in}}, K^{\text{out}}}$, can be generated by adapting the standard

stub matching procedure [7] to directed graphs. First, we draw a sequence of indegrees $(K_1^{\text{in}}, K_2^{\text{in}}, \dots, K_n^{\text{in}})$ and outdegrees $(K_1^{\text{out}}, K_2^{\text{out}}, \dots, K_n^{\text{out}})$ from the distribution $p_{K^{\text{in}}, K^{\text{out}}}$, Eq. (S1), conditioned by the constraint $\sum_{j=1}^n K_j^{\text{in}} = \sum_{j=1}^n K_j^{\text{out}}$. Second, we assign a total number of K_i^{out} outward stubs and K_i^{in} inward stubs to each node i ($i = 1, \dots, N$). A pair of stubs, containing an outward stub and an inward stub, is selected at random with uniform probability and then connected to create a directed edge between a pair of nodes. The corresponding entry of the adjacency matrix \mathbf{A} is set to a value drawn from the distribution of weights p_J . This stub matching process is repeated until there are no remainder stubs and a simple graph is returned, i.e., graph instances containing self-edges or multiedges are rejected. This procedure generates directed random graphs that are uniformly sampled from the space of simple graphs. We point out that, although we only consider simple graphs, the results for the spectral properties of \mathbf{A} presented in this paper should also apply to the configuration model of directed graphs with multiedges and self-edges. The main reason is that the fraction of multiedges and self-edges vanishes when $N \rightarrow \infty$ [4], provided the ratio c/N goes to zero as $N \rightarrow \infty$. The latter condition is satisfied if c scales very slowly with N .

Because nodes are connected in a random fashion, the local neighbourhood of a randomly selected node is with probability one locally tree-like and oriented in the limit $n \rightarrow \infty$. The oriented property means that all edges are unidirectional. The relevance of the oriented property and the local tree-like structure of the graph to the derivation of Eq. (7) in the main text has been discussed in previous works [8, 9].

Below we present some properties of four examples of degree distributions, namely, regular, Poisson, exponential, and Borel distributions. The properties of these distributions are important to reproduce and understand some of the results in the main text. We will only specify the outdegree distribution $p_{K^{\text{out}}}(k)$, since $p_{K^{\text{out}}} = (k)p_{K^{\text{in}}}(k)$ in each case.

A. Regular graphs

In the c -regular ensemble, the indegree and outdegree of each node is equal to a constant c [10], such that

$$p_{K^{\text{out}}}(k) = p_{K^{\text{in}}}(k) = \delta_{k,c}, \quad (\text{S2})$$

where δ is the Kronecker delta function. The moments of $p_{K^{\text{out}}}(k)$ read

$$\langle (K^{\text{out}})^n \rangle = c^n, \quad n \geq 1, \quad (\text{S3})$$

while the variance of the outdegree distribution is given by

$$\text{var}[K^{\text{out}}] = 0. \quad (\text{S4})$$

B. Poisson graphs

For this ensemble, the degree distribution is given by

$$p_{K^{\text{out}}}(k) = \frac{e^{-c} c^k}{k!}, \quad (\text{S5})$$

where $c > 0$ is a real parameter. Analytic expressions for the moments follow from the generating function

$$g(x) = \sum_{k=0}^{\infty} p_{K^{\text{out}}}(k) e^{xk} = e^{c(e^x - 1)} \quad (\text{S6})$$

through the derivatives

$$\langle (K^{\text{out}})^n \rangle = \left. \frac{d^n g}{dx^n} \right|_{x=0}. \quad (\text{S7})$$

In the main text of the paper, we need the first four moments

$$\begin{aligned} \langle K^{\text{out}} \rangle &= c, \\ \langle (K^{\text{out}})^2 \rangle &= c(c+1), \\ \langle (K^{\text{out}})^3 \rangle &= c(c+1) + c^2(c+2), \\ \langle (K^{\text{out}})^4 \rangle &= c(c+1) + 3c^2(c+2) + c^3(c+3). \end{aligned} \quad (\text{S8})$$

The variance of the outdegree distribution is

$$\text{var}[K^{\text{out}}] = c. \quad (\text{S9})$$

C. Exponential graphs

For exponential graphs, the degree distribution is

$$p_{K^{\text{out}}}(k) = \frac{1}{c+1} \left(\frac{c}{c+1} \right)^k, \quad (\text{S10})$$

with $c > 0$. By making the change of variables $x \equiv \ln\left(\frac{c}{c+1}\right)$, the n -moment can be computed from the equation

$$\langle (K^{\text{out}})^n \rangle = \frac{1}{c+1} \sum_{k=0}^{\infty} k^n e^{xk} = \frac{1}{c+1} \left[\frac{d^n}{dx^n} \frac{1}{1 - e^x} \right] \bigg|_{x=\ln\left(\frac{c}{c+1}\right)}. \quad (\text{S11})$$

The analytic expressions for the first four moments read

$$\begin{aligned}\langle K^{\text{out}} \rangle &= c, \\ \langle (K^{\text{out}})^2 \rangle &= 2c^2 + c, \\ \langle (K^{\text{out}})^3 \rangle &= 6c^3 + 6c^2 + c, \\ \langle (K^{\text{out}})^4 \rangle &= 24c^4 + 36c^3 + 14c^2 + c,\end{aligned}$$

and the variance is given by

$$\text{var}[K^{\text{out}}] = c^2 + c. \quad (\text{S12})$$

D. Borel graphs

In these graphs $p_{K^{\text{out}}}(k)$ follows a Borel distribution. The Borel distribution is defined as [11, 12]

$$p_{K^{\text{out}}}(k) = \frac{e^{-\mu k} (\mu k)^{k-1}}{k!}, \quad (\text{S13})$$

where k is a positive integer and $\mu \in [0, 1]$ is a control parameter. As far as we are aware, the Borel degree distribution has not been considered in the context of random networks, thus we discuss in more detail the calculation of the moments in this case.

The moments of the Borel distribution can be evaluated in a recursive way. Here we lay out this recursive approach explicitly for the first two moments, while the third and the fourth moments follow through a similar calculation which we do not present explicitly. We use the change of variables

$$\nu \equiv \mu e^{-\mu} \quad (\text{S14})$$

in the normalization condition $\sum_{k=1}^{\infty} p_{K^{\text{out}}}(k) = 1$ to obtain the useful identity

$$\sum_{k=1}^{\infty} \frac{k^{k-1} \nu^k}{k!} = \mu. \quad (\text{S15})$$

We first address how μ is related to the mean outdegree

$$c = \langle K^{\text{out}} \rangle. \quad (\text{S16})$$

We take the derivative of Eq. (S15) with respect to ν and obtain

$$c = \frac{\nu}{\mu} \frac{d\mu}{d\nu}. \quad (\text{S17})$$

The derivative $\frac{d\mu}{d\nu}$ follows from Eq. (S14), namely,

$$\frac{d\mu}{d\nu} = \frac{e^\mu}{1-\mu}. \quad (\text{S18})$$

Substituting Eqs. (S14) and (S18) in Eq. (S17) leads to

$$c = \frac{1}{1-\mu}. \quad (\text{S19})$$

Hence, analogously to the Poisson and exponential outdegree distributions, $p_{K^{\text{out}}}(k)$ is parametrized solely by the mean outdegree c through the relation (S19). The limit $\mu \rightarrow 1$ corresponds to the high connectivity limit $c \rightarrow \infty$, while $\mu \rightarrow 0$ yields $c \rightarrow 1$.

The second moment of the outdegree distribution is given by

$$\langle (K^{\text{out}})^2 \rangle = \sum_{k=1}^{\infty} k^2 p_{K^{\text{out}}}(k) = \sum_{k=1}^{\infty} \frac{k^{k+1} \nu^k}{\mu k!}. \quad (\text{S20})$$

By taking a second order derivative of Eq. (S15) with respect to ν and using the above equation, we obtain

$$\langle (K^{\text{out}})^2 \rangle = \frac{\nu^2}{\mu} \frac{d^2 \mu}{d\nu^2} + c. \quad (\text{S21})$$

The expression for $\frac{d^2 \mu}{d\nu^2}$ is obtained from taking the derivative of Eq. (S18) with respect to ν , namely,

$$\frac{d^2 \mu}{d\nu^2} = \frac{e^{2\mu}(2-\mu)}{(1-\mu)^3}. \quad (\text{S22})$$

We get the analytic expression for $\langle (K^{\text{out}})^2 \rangle$ by plugging the above equation back in Eq. (S21), yielding

$$\langle (K^{\text{out}})^2 \rangle = \frac{1}{(1-\mu)^3}. \quad (\text{S23})$$

The third and fourth moments of $p_{K^{\text{out}}}(k)$ are computed following the same recursive approach. The final analytic expressions are given by

$$\langle (K^{\text{out}})^3 \rangle = \frac{1+2\mu}{(1-\mu)^5} \quad (\text{S24})$$

and

$$\langle (K^{\text{out}})^4 \rangle = \frac{-12\mu^3 + 24\mu^2 + 8\mu - 5}{(1-\mu)^7}. \quad (\text{S25})$$

The variance of the Borel outdegree distribution reads

$$\text{var}[K^{\text{out}}] = c^3 - c^2. \quad (\text{S26})$$

E. Comparing the degree distributions

The four outdegree distributions introduced above have finite moments and are parametrized by a single parameter, namely the mean outdegree c . For a fixed c , we can compare four outdegree distributions with the same mean c but different variances. Thus, we use these four degree distributions to illustrate how degree fluctuations affect the localization and the universality properties of the eigenvectors of directed random graphs.

Figure S1 shows the Poisson, the exponential, and the Borel outdegree distributions for $c = 5$. The Borel distribution $p_{K^{\text{out}}}(k)$ decays slower for $k \gg 1$ in comparison to the other distributions, i.e., the probability of having nodes with large outdegree k is higher for the Borel distribution than for regular, Poisson, and exponential distributions.

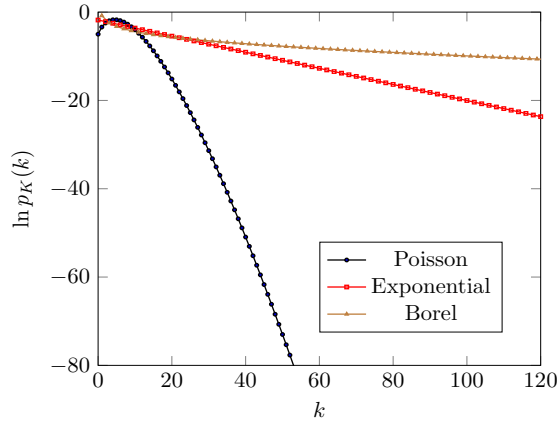


FIG. S1: Poisson, exponential, and Borel outdegree distributions $p_{K^{\text{out}}}(k)$ for $c = 5$ (see Eqs. (S5), (S10), and (S13)). The y -axis displays the logarithm of $p_{K^{\text{out}}}(k)$ to highlight the difference in the tails of the distributions.

The strength of the degree fluctuations of the four ensembles is also captured by the scaling of the variance $\sigma_{K^{\text{out}}}^2$ with $c \gg 1$. In all four cases, the variance of K^{out} scales as

$$\text{var}[K^{\text{out}}] = Bc^\alpha, \quad (\text{S27})$$

for $c \gg 1$. In particular, for regular graphs $\alpha \rightarrow -\infty$, for Poisson graphs $\alpha = 1$, for exponential graphs $\alpha = 2$, and for Borelian graphs $\alpha = 3$. According to Eqs. (15) and (16) in the main text, the different universal behaviors of the right eigenvector distributions for $c \rightarrow \infty$ can be classified in terms of the asymptotic behaviour of the relative variance

$\text{var}[K^{\text{out}}]/c^2$, which is essentially controlled by the exponent α . The parameter $\text{var}[K^{\text{out}}]/c^2$ vanishes for regular random graphs and for the Poisson distribution (both models have $\alpha < 2$), $\text{var}[K^{\text{out}}]/c^2$ diverges for the Borel distribution ($\alpha > 2$), and $\text{var}[K^{\text{out}}]/c^2$ remains finite for the exponential distribution ($\alpha = 2$). In the marginal case of $\alpha = 2$, the high connectivity limit of the eigenvector distribution is determined by the prefactor B ($B = 1$ for the exponential distribution). Each of the outdegree distributions discussed here provides an example of a network ensemble within a certain universality class (see also table I in the main text).

S3. CALCULATION OF THE INVERSE PARTICIPATION RATIO

We derive Eqs. (9) and (10) in the main text for the inverse participation ratio (IPR) of the right eigenvectors associated to the outlier λ_{isol} and to an eigenvalue λ_{b} at the boundary of the spectral distribution $\rho_{\mathbf{A}}(\lambda)$. We restrict ourselves to right eigenvectors since the results for left eigenvectors are obtained through the substitution “out \rightarrow in”. The IPR $\mathcal{I}(\lambda)$ of a right eigenvector $\vec{R}(\lambda)$ is determined from (see also Eq. (8) in the main text)

$$\mathcal{I}(\lambda) = \frac{\langle |R(\lambda)|^4 \rangle}{\langle |R(\lambda)|^2 \rangle^2}. \quad (\text{S28})$$

Below we show how to compute the moments $\langle |R(\lambda)|^2 \rangle$ and $\langle |R(\lambda)|^4 \rangle$ of the distribution p_R of the right eigenvector components.

A. Moments of p_R

As shown in Refs. [8, 13], the limit $n \rightarrow \infty$ of the distribution $p_R(r|\lambda)$ of the right eigenvector components associated to an eigenvalue $\lambda = \lambda_{\text{isol}}$ or $\lambda = \lambda_{\text{b}}$ solves the distributional Eq. (7) in the main text

$$p_R(r|\lambda) = \sum_{k=0}^{\infty} p_{K^{\text{out}}}(k) \int \left(\prod_{j=1}^k dx_j d^2 r_j p_J(x_j) p_R(r_j|\lambda) \right) \delta \left(r - \frac{1}{\lambda} \sum_{j=1}^k x_j r_j \right). \quad (\text{S29})$$

The $m + n$ -moment of p_R is given by

$$\langle R^n (R^*)^m \rangle = \int d^2 r p_R(r|\lambda) r^n (r^*)^m. \quad (\text{S30})$$

Inserting Eq. (S29) in Eq. (S30) yields

$$\langle R^n (R^*)^m \rangle = \frac{1}{\lambda^n (\lambda^*)^m} \sum_{k=0}^{\infty} p_{K^{\text{out}}}(k) \int \left(\prod_{j=1}^k dx_j d^2 r_j p_J(x_j) p_R(r_j | \lambda) \right) \left(\sum_{j=1}^k x_j r_j \right)^n \left(\sum_{j=1}^k x_j r_j^* \right)^m. \quad (\text{S31})$$

Using the multinomial theorem, we can rewrite the above expression as

$$\begin{aligned} \langle R^n (R^*)^m \rangle &= \frac{1}{\lambda^n (\lambda^*)^m} \sum_{k=0}^{\infty} p_{K^{\text{out}}}(k) \sum_{i_1 + \dots + i_k = n} \sum_{j_1 + \dots + j_k = m} C_n(i_1, \dots, i_k) C_m(j_1, \dots, j_k) \\ &\times \prod_{t=1}^k \langle J_t^{i_t + j_t} \rangle \prod_{t=1}^k \langle R_t^{i_t} (R_t^*)^{j_t} \rangle, \end{aligned} \quad (\text{S32})$$

with the coefficients

$$C_n(i_1, \dots, i_k) = \frac{n!}{\prod_{t=1}^k i_t!}, \quad \text{and} \quad C_m(j_1, \dots, j_k) = \frac{m!}{\prod_{t=1}^k j_t!}. \quad (\text{S33})$$

The sum $\sum_{i_1 + \dots + i_k = n} (\sum_{j_1 + \dots + j_k = m})$ runs over all distinct combinations of non-negative integers i_1, \dots, i_k (j_1, \dots, j_k) such that $\sum_{t=1}^k i_t = n$ ($\sum_{t=1}^k j_t = m$). Equation (S32) allows to calculate recursively the moments of p_R , as we demonstrate below.

B. The eigenvalue outlier λ_{isol} and eigenvalues λ_b at the boundary of the spectrum

By setting $n = 1$ and $m = 0$ in Eq. (S32), we obtain the fixed-point equation for the mean $\langle R \rangle$

$$\langle R \rangle = \frac{c \langle J \rangle}{\lambda} \langle R \rangle. \quad (\text{S34})$$

Analogously, we can set $n = m = 1$ in Eq. (S32) yielding

$$|\lambda|^2 \langle |R|^2 \rangle = c \langle J^2 \rangle \langle |R|^2 \rangle + \langle K^{\text{out}} (K^{\text{out}} - 1) \rangle \langle J \rangle^2 \langle |R|^2 \rangle. \quad (\text{S35})$$

For $n = 2$ and $m = 0$ we get

$$\lambda^2 \langle R^2 \rangle = c \langle J^2 \rangle \langle R^2 \rangle + \langle K^{\text{out}} (K^{\text{out}} - 1) \rangle \langle J \rangle^2 \langle R \rangle^2. \quad (\text{S36})$$

If $\langle R \rangle \neq 0$, then

$$\lambda = \lambda_{\text{isol}} = c \langle J \rangle, \quad (\text{S37})$$

which is the eigenvalue outlier. On the other hand, if $\langle R \rangle = 0$, then

$$\langle |R|^2 \rangle = \frac{c \langle J^2 \rangle}{|\lambda|^2} \langle |R|^2 \rangle, \quad (\text{S38})$$

leading to

$$|\lambda^2| = |\lambda_b^2| = c\langle J^2 \rangle, \quad (\text{S39})$$

which is the boundary of the spectrum.

C. The IPR for the right eigenvector associated to an eigenvalue λ_b

The IPR is the ratio between the fourth moment and the second moment of $p_R(r|\lambda)$ (see Eq. (8) in the main text). In this subsection we calculate the IPR for the right eigenvectors associated to λ_b , for which $\langle R \rangle = 0$. We need to distinguish between $\lambda_b \in \mathbb{R}$ and $\lambda_b \notin \mathbb{R}$ as the distribution p_R is different in each case. This follows from the fact that $\vec{R}(\lambda)$ only contains real components when $\lambda \in \mathbb{R}$.

We first analyze the second moments of p_R . If $\lambda_b \notin \mathbb{R}$, then Eq. (S36) implies that $\langle R^2 \rangle = 0$, while for $\lambda_b \in \mathbb{R}$ we have that $\langle R^2 \rangle = \langle |R|^2 \rangle \neq 0$. We do not need to compute $\langle |R|^2 \rangle$, since its value is determined by the choice of normalization for the right eigenvectors.

The third moments $\langle R^3 \rangle$ and $\langle R^2 R^* \rangle$ are obtained from Eq. (S32) when $n + m = 3$. By inspecting the different terms in Eq. (S32) and taking into account that $\langle R \rangle = \langle R^* \rangle = 0$, we conclude that the third moments solve the linear equations

$$\langle R^3 \rangle = \frac{c\langle J^3 \rangle}{\lambda_b^3} \langle R^3 \rangle, \quad (\text{S40})$$

$$\langle R^2 R^* \rangle = \frac{c\langle J^3 \rangle}{\lambda_b^2 \lambda_b^*} \langle R^2 R^* \rangle. \quad (\text{S41})$$

Since $|\lambda_b|^2 = c\langle J^2 \rangle$, it holds that $\langle R^3 \rangle = \langle R^2 R^* \rangle = 0$ for both $\lambda_b \in \mathbb{R}$ and $\lambda_b \notin \mathbb{R}$.

Lastly, we compute the fourth moments of p_R . If $\lambda_b \in \mathbb{R}$, then we are only concerned with a single fourth moment since $\langle |R|^4 \rangle = \langle R^4 \rangle = \langle R^3 R^* \rangle$. In this case, we set $n = 4$ and $m = 0$ in Eq. (S32), and use the fact that the first and the third moments of p_R are zero, which yields

$$\begin{aligned} \langle R^4 \rangle &= \frac{1}{\lambda_b^4} \sum_{k=0}^{\infty} p_{K^{\text{out}}}(k) \left[k \langle J^4 \rangle \langle R^4 \rangle + \frac{k(k-1)}{2} \frac{4!}{2!2!} \langle J^2 \rangle^2 \langle R^2 \rangle^2 \right] \\ &= \frac{1}{\lambda_b^4} [c \langle J^4 \rangle \langle R^4 \rangle + 3 \langle K^{\text{out}}(K^{\text{out}} - 1) \rangle \langle J^2 \rangle^2 \langle R^2 \rangle^2]. \end{aligned} \quad (\text{S42})$$

Using that $\lambda_b = \sqrt{c\langle J^2 \rangle}$ in the above expression, we readily obtain from Eq. (S28) the

analytic expression for the IPR

$$\mathcal{I}(\lambda_b) = \frac{3\langle J^2 \rangle^2 \langle K^{\text{out}}(K^{\text{out}} - 1) \rangle}{c(c\langle J^2 \rangle^2 - \langle J^4 \rangle)}, \quad (\text{S43})$$

which is the Eq. (9) in the main text for $\gamma = 2$.

If $\lambda = \lambda_b \notin \mathbb{R}$, then we have to consider three different combinations of n and m in Eq. (S32) that yield fourth moments ($n + m = 4$): $\langle R^4 \rangle$, $\langle R^3 R^* \rangle$, and $\langle |R|^4 \rangle$. Since $\langle R \rangle = \langle R^2 \rangle = 0$ for $\lambda_b \notin \mathbb{R}$ in the multinomial expansion of Eq. (S32), one obtains that $\langle R^3 R^* \rangle$ and $\langle R^4 \rangle$ are determined from the solutions of two linear equations, which have a structure similar to Eqs. (S40) and (S41). From these linear equations for $\langle R^3 R^* \rangle$ and $\langle R^4 \rangle$, it is straightforward to verify that $\langle R^3 R^* \rangle = \langle R^4 \rangle = 0$ when $|\lambda| = \sqrt{c\langle J^2 \rangle}$. We are thus left with a single fourth moment to compute, namely $\langle |R|^4 \rangle$. Setting $n = m = 2$ and $\lambda = \lambda_b \notin \mathbb{R}$ in Eq. (S32), we get

$$\begin{aligned} \langle |R|^4 \rangle &= \frac{1}{|\lambda_b|^4} \sum_{k=0}^{\infty} p_{K^{\text{out}}}(k) \left[k \langle J^4 \rangle \langle |R|^4 \rangle + \frac{1}{2} k(k-1) 2! 2! \langle J^2 \rangle^2 \langle |R|^2 \rangle^2 \right] \\ &= \frac{1}{|\lambda_b|^4} [c \langle J^4 \rangle \langle |R|^4 \rangle + 2 \langle K^{\text{out}}(K^{\text{out}} - 1) \rangle \langle J^2 \rangle^2 \langle |R|^2 \rangle^2]. \end{aligned} \quad (\text{S44})$$

Substituting $|\lambda_b| = \sqrt{c\langle J^2 \rangle}$ in the above equation, we obtain from Eq. (S28) the analytic expression for the IPR

$$\mathcal{I}(\lambda_b) = \frac{\langle |R|^4 \rangle}{\langle |R|^2 \rangle^2} = \frac{2\langle J^2 \rangle^2 \langle K^{\text{out}}(K^{\text{out}} - 1) \rangle}{c(c\langle J^2 \rangle^2 - \langle J^4 \rangle)}, \quad (\text{S45})$$

which is the Eq. (9) for $\gamma = 1$.

The only difference between Eqs. (S43) and (S45) is the numerical factor in the numerator, and therefore we can write

$$\frac{\langle |R|^4 \rangle}{\langle |R|^2 \rangle^2} = \frac{(\gamma + 1) \langle J^2 \rangle^2 \langle K^{\text{out}}(K^{\text{out}} - 1) \rangle}{c(c\langle J^2 \rangle^2 - \langle J^4 \rangle)}, \quad (\text{S46})$$

where $\gamma = 2$ if $\lambda_b \in \mathbb{R}$, and $\gamma = 1$ if $\lambda_b \notin \mathbb{R}$.

D. The IPR for the right eigenvector associated to the outlier eigenvalue λ_{isol}

In this subsection we compute the IPR of the right eigenvector associated to the outlier eigenvalue λ_{isol} . Since $\langle R \rangle \neq 0$, the odd moments of p_R are nonzero and the calculation

of the IPR is more involved than for $\lambda = \lambda_b$. Substituting $\lambda = \lambda_{\text{isol}} = c\langle J \rangle$ in Eq. (S36), we readily obtain the analytic expression [8]

$$\frac{\langle R^2 \rangle}{\langle R \rangle^2} = \frac{\langle J \rangle^2 \langle K^{\text{out}}(K^{\text{out}} - 1) \rangle}{c(c\langle J \rangle^2 - \langle J^2 \rangle)}. \quad (\text{S47})$$

Note that the right hand side of the above equation is positive only if $c > c_{\text{gap}} = \langle J^2 \rangle / \langle J \rangle^2$, which is the condition for the existence of an outlier (see Eq. (4) in the main text). As before, the value of $\langle R^2 \rangle$ is determined by the choice of the eigenvector normalization.

Combining Eqs. (S47) and (S32), we can calculate the third moment $\langle R^3 \rangle$. Setting $\lambda = \lambda_{\text{isol}}$, $n = 3$, and $m = 0$ in Eq. (S32), we find

$$\begin{aligned} \langle R^3 \rangle &= \frac{1}{\lambda_{\text{isol}}^3} \sum_{k=0}^{\infty} p_{K^{\text{out}}}(k) \left[k \langle J^3 \rangle \langle R^3 \rangle + 3k(k-1) \langle J^2 \rangle \langle J \rangle \langle R^2 \rangle \langle R \rangle + \frac{k!}{(k-3)!} \langle J \rangle^3 \langle R \rangle^3 \right] \\ &= \frac{1}{\lambda_{\text{isol}}^3} \left[c \langle J^3 \rangle \langle R^3 \rangle + 3 \langle K^{\text{out}}(K^{\text{out}} - 1) \rangle \langle J^2 \rangle \langle J \rangle \langle R^2 \rangle \langle R \rangle \right. \\ &\quad \left. + \langle K^{\text{out}}(K^{\text{out}} - 1)(K^{\text{out}} - 2) \rangle \langle J \rangle^3 \langle R \rangle^3 \right], \end{aligned} \quad (\text{S48})$$

where the combinatorial factor $\frac{k!}{(k-3)!}$ is equal to the number of distinct k -dimensional vectors with $k-3$ components equal to zero and three components equal to one. Using $\lambda_{\text{isol}} = c\langle J \rangle$ and dividing the above equation by $\langle R \rangle^3$, leads to

$$(c^3 \langle J \rangle^3 - c \langle J^3 \rangle) \frac{\langle R^3 \rangle}{\langle R \rangle^3} = 3 \langle K^{\text{out}}(K^{\text{out}} - 1) \rangle \langle J^2 \rangle \langle J \rangle \frac{\langle R^2 \rangle}{\langle R \rangle^2} + \langle K^{\text{out}}(K^{\text{out}} - 1)(K^{\text{out}} - 2) \rangle \langle J \rangle^3. \quad (\text{S49})$$

Inserting Eq. (S47) in Eq. (S49), we obtain that the third moment is given by

$$\frac{\langle R^3 \rangle}{\langle R \rangle^3} = \frac{3 \langle K^{\text{out}}(K^{\text{out}} - 1) \rangle^2 \langle J \rangle^3 \langle J^2 \rangle}{(c^3 \langle J \rangle^3 - c \langle J^3 \rangle)(c^2 \langle J \rangle^2 - c \langle J^2 \rangle)} + \frac{\langle K^{\text{out}}(K^{\text{out}} - 1)(K^{\text{out}} - 2) \rangle \langle J \rangle^3}{(c^3 \langle J \rangle^3 - c \langle J^3 \rangle)}. \quad (\text{S50})$$

Lastly, we compute the fourth moment of p_R from the multinomial expansion of Eq. (S32) for $n = 4$ and $m = 0$. The computation is more involved and we need to be careful and take properly into account all combinatorial factors. There are five different types of configurations of non-negative integers i_1, \dots, i_k that fulfill the constraint $\sum_{t=1}^k i_t = 4$. Below we show a single instance of i_1, \dots, i_k belonging to each type, together with the combinatorial factor arising from taking all possible permutations of a certain configuration

type:

$$\begin{aligned}
i_1 = 4 \quad i_2 = \dots = i_k = 0 &\longrightarrow k, \\
i_1 = i_2 = i_3 = i_4 = 1 \quad i_5 = \dots = i_k = 0 &\longrightarrow \frac{k!}{4!(k-4)!}, \\
i_1 = 3, i_2 = 1 \quad i_3 = \dots = i_k = 0 &\longrightarrow k(k-1), \\
i_1 = i_2 = 2 \quad i_3 = \dots = i_k = 0 &\longrightarrow \frac{k(k-1)}{2}, \\
i_1 = 2, i_2 = i_3 = 1 \quad i_4 = \dots = i_k = 0 &\longrightarrow \frac{k(k-1)(k-2)}{2}.
\end{aligned}$$

Taking into account the above combinatorial factors, Eq. (S32) assumes the form

$$\begin{aligned}
\langle R^4 \rangle &= \frac{1}{\lambda_{\text{isol}}^4} \sum_{k=0}^{\infty} p_{K^{\text{out}}}(k) \left[k \langle J^4 \rangle \langle R^4 \rangle + k(k-1)(k-2)(k-3) \langle J \rangle^4 \langle R \rangle^4 \right. \\
&\quad + 4k(k-1) \langle J^3 \rangle \langle J \rangle \langle R^3 \rangle \langle R \rangle \\
&\quad + 3k(k-1) \langle J^2 \rangle^2 \langle R^2 \rangle^2 + 6k(k-1)(k-2) \langle J^2 \rangle \langle J \rangle^2 \langle R^2 \rangle \langle R \rangle^2 \Big], \\
&= \frac{1}{\lambda_{\text{isol}}^4} \left[c \langle J^4 \rangle \langle R^4 \rangle + \langle K^{\text{out}}(K^{\text{out}}-1)(K^{\text{out}}-2)(K^{\text{out}}-3) \rangle \langle J \rangle^4 \langle R \rangle^4 \right. \\
&\quad + 4 \langle K^{\text{out}}(K^{\text{out}}-1) \rangle \langle J^3 \rangle \langle J \rangle \langle R^3 \rangle \langle R \rangle \\
&\quad + 3 \langle K^{\text{out}}(K^{\text{out}}-1) \rangle \langle J^2 \rangle^2 \langle R^2 \rangle^2 + 6 \langle K^{\text{out}}(K^{\text{out}}-1)(K^{\text{out}}-2) \rangle \langle J^2 \rangle \langle J \rangle^2 \langle R^2 \rangle \langle R \rangle^2 \Big].
\end{aligned}$$

Substituting $\lambda_{\text{isol}} = c \langle J \rangle$ and dividing the above equation by $\langle R \rangle^4$, we arrive at

$$\begin{aligned}
(c^4 \langle J \rangle^4 - c \langle J^4 \rangle) \frac{\langle R^4 \rangle}{\langle R \rangle^4} &= \langle K^{\text{out}}(K^{\text{out}}-1)(K^{\text{out}}-2)(K^{\text{out}}-3) \rangle \langle J \rangle^4 \\
&\quad + 4 \langle K^{\text{out}}(K^{\text{out}}-1) \rangle \langle J^3 \rangle \langle J \rangle \frac{\langle R^3 \rangle}{\langle R \rangle^3} + 3 \langle K^{\text{out}}(K^{\text{out}}-1) \rangle \langle J^2 \rangle^2 \frac{\langle R^2 \rangle^2}{\langle R \rangle^4} \\
&\quad + 6 \langle K^{\text{out}}(K^{\text{out}}-1)(K^{\text{out}}-2) \rangle \langle J^2 \rangle \langle J \rangle^2 \frac{\langle R^2 \rangle}{\langle R \rangle^2}.
\end{aligned}$$

The analytic expression for $\frac{\langle R^4 \rangle}{\langle R \rangle^4}$ is derived by substituting Eqs. (S47) and (S50) in the above equation leading to

$$\begin{aligned}
\frac{\langle R^4 \rangle}{\langle R \rangle^4} &= \frac{\langle K^{\text{out}}(K^{\text{out}}-1)(K^{\text{out}}-2)(K^{\text{out}}-3) \rangle \langle J \rangle^4}{(c^4 \langle J \rangle^4 - c \langle J^4 \rangle)} \\
&\quad + \frac{12 \langle K^{\text{out}}(K^{\text{out}}-1) \rangle^3 \langle J \rangle^4 \langle J^3 \rangle \langle J^2 \rangle}{(c^4 \langle J \rangle^4 - c \langle J^4 \rangle) (c^3 \langle J \rangle^3 - c \langle J^3 \rangle) (c^2 \langle J \rangle^2 - c \langle J^2 \rangle)} \\
&\quad + \frac{4 \langle K^{\text{out}}(K^{\text{out}}-1) \rangle \langle K^{\text{out}}(K^{\text{out}}-1)(K^{\text{out}}-2) \rangle \langle J \rangle^4 \langle J^3 \rangle}{(c^4 \langle J \rangle^4 - c \langle J^4 \rangle) (c^3 \langle J \rangle^3 - c \langle J^3 \rangle)} \\
&\quad + \frac{3 \langle K^{\text{out}}(K^{\text{out}}-1) \rangle^3 \langle J^2 \rangle^2 \langle J \rangle^4}{(c^4 \langle J \rangle^4 - c \langle J^4 \rangle) (c^2 \langle J \rangle^2 - c \langle J^2 \rangle)^2} \\
&\quad + \frac{6 \langle K^{\text{out}}(K^{\text{out}}-1)(K^{\text{out}}-2) \rangle \langle K^{\text{out}}(K^{\text{out}}-1) \rangle \langle J^2 \rangle \langle J \rangle^4}{(c^4 \langle J \rangle^4 - c \langle J^4 \rangle) (c^2 \langle J \rangle^2 - c \langle J^2 \rangle)}. \tag{S51}
\end{aligned}$$

The IPR follows from Eq. (S28) (see also Eq. (8) in the main text). Using Eq. (S47), we express $\langle R \rangle^4$ in terms of $\langle R^2 \rangle^2$, obtaining the following analytic expression for the IPR of the right eigenvector associated to λ_{isol} (see Eq. (10) in the main text)

$$\begin{aligned} \frac{\langle R^4 \rangle}{\langle R^2 \rangle^2} &= \frac{3\beta_1 \langle J^2 \rangle^2}{(c^4 \langle J \rangle^4 - c \langle J^4 \rangle)} + \frac{\beta_3 (c^2 \langle J \rangle^2 - c \langle J^2 \rangle)^2}{\beta_1^2 (c^4 \langle J \rangle^4 - c \langle J^4 \rangle)} + \frac{12\beta_1 \langle J^3 \rangle \langle J^2 \rangle (c^2 \langle J \rangle^2 - c \langle J^2 \rangle)}{(c^4 \langle J \rangle^4 - c \langle J^4 \rangle) (c^3 \langle J \rangle^3 - c \langle J^3 \rangle)} \\ &+ \frac{4\beta_2 \langle J^3 \rangle (c^2 \langle J \rangle^2 - c \langle J^2 \rangle)^2}{\beta_1 (c^4 \langle J \rangle^4 - c \langle J^4 \rangle) (c^3 \langle J \rangle^3 - c \langle J^3 \rangle)} + \frac{6\beta_2 \langle J^2 \rangle (c^2 \langle J \rangle^2 - c \langle J^2 \rangle)}{\beta_1 (c^4 \langle J \rangle^4 - c \langle J^4 \rangle)}, \end{aligned} \quad (\text{S52})$$

where the coefficients β_ℓ ($\ell = 1, 2, 3$) depend solely on the outdegree distribution and are defined as

$$\beta_\ell = \sum_{k=\ell+1}^{\infty} p_{K^{\text{out}}}(k) \frac{k!}{(k-\ell-1)!}. \quad (\text{S53})$$

S4. THE HIGH CONNECTIVITY LIMIT FOR THE DISTRIBUTION OF EIGENVECTOR COMPONENTS

In this section, we derive the analytic expressions for the high connectivity limit $c \rightarrow \infty$ of $p_R(r|\lambda)$ given by Eqs. (22)-(25) in the main text. We consider explicitly the cases of regular, Poisson, and exponential random graphs, and we discuss why the approach presented here does not work for random graphs with Borel degree distributions.

A. General formalism

In general, the eigenvector components are complex random variables and $p_R(r|\lambda)$ represents the joint distribution of the real and imaginary components ($\text{Re}(R), \text{Im}(R)$) in the complex plane. We consider the characteristic function

$$g_R(u, v|\lambda) = \int d^2r p_R(r|\lambda) e^{-iu\text{Re}(r) - iv\text{Im}(r)} \quad (\text{S54})$$

of $p_R(r|\lambda)$, where $d^2r \equiv d\text{Re}(r)d\text{Im}(r)$ and the integral is over the complex plane. If we know the analytic expression for $g_R(u, v|\lambda)$, we obtain $p_R(r|\lambda)$ from

$$p_R(r|\lambda) = \int \frac{dudv}{4\pi^2} e^{iu\text{Re}(r) + iv\text{Im}(r)} g_R(u, v|\lambda). \quad (\text{S55})$$

In what follows, we compute $g_R(u, v|\lambda)$ in the limit $c \rightarrow \infty$, which is then substituted in the above equation to obtain $p_R(r|\lambda)$.

First, we rewrite $g_R(u, v|\lambda)$ by substituting Eq. (S29) in Eq. (S54), yielding

$$\begin{aligned} g_R(u, v|\lambda) &= \sum_{k=0}^{\infty} p_{K^{\text{out}}}(k) \int \left(\prod_{j=1}^k dx_j d^2 r_j p_J(x_j) p_R(r_j|\lambda) \right) \\ &\quad \times \exp \left[-iu \sum_{j=1}^k x_j \text{Re} \left(\frac{r_j}{\lambda} \right) - iv \sum_{j=1}^k x_j \text{Im} \left(\frac{r_j}{\lambda} \right) \right] \\ &= \sum_{k=0}^{\infty} p_{K^{\text{out}}}(k) \exp [k \ln F(u, v|\lambda)]. \end{aligned} \quad (\text{S56})$$

If $\lambda \in \mathbb{C}$, then the eigenvector components are complex and the function $F(u, v|\lambda)$ is given by

$$F(u, v|\lambda \in \mathbb{C}) = \int dx p_J(x) \int d^2 r p_R(r) \exp \left(-\frac{xzr}{2\lambda} + \frac{xz^*r^*}{2\lambda^*} \right), \quad (\text{S57})$$

with $z \equiv u + iv$, and where $(\dots)^*$ denotes complex conjugation. On the other hand, if $\lambda \in \mathbb{R}$, then the eigenvector components are distributed on the real line and $F(u, v|\lambda)$ is independent of v , i.e.,

$$F(u|\lambda \in \mathbb{R}) = \int dx p_J(x) \int d^2 r p_R(r) \exp \left(-\frac{iuxr}{\lambda} \right). \quad (\text{S58})$$

In order to compute the high connectivity limit $c \rightarrow \infty$ of g_R , we expand F in powers of $1/c$ for $c \gg 1$. By representing the exponential in Eqs. (S57) and (S58) as power-series, we obtain the formal expressions

$$F(u, v|\lambda \in \mathbb{C}) = \sum_{n,m=0}^{\infty} \frac{1}{n!m!} \left(-\frac{z}{2} \right)^n \left(\frac{z^*}{2} \right)^m \frac{\langle J^{n+m} \rangle}{\lambda^n (\lambda^*)^m} \langle R^n (R^*)^m \rangle, \quad (\text{S59})$$

$$F(u|\lambda \in \mathbb{R}) = \sum_{n=0}^{\infty} \frac{(-iu)^n}{n!} \frac{\langle J^n \rangle}{\lambda^n} \langle R^n \rangle. \quad (\text{S60})$$

Substituting the values $\lambda = \lambda_{\text{isol}} = c\langle J \rangle$ or $|\lambda|^2 = |\lambda_{\text{b}}|^2 = c\langle J^2 \rangle$ in Eqs. (S59-S60), we obtain expansions in powers of $1/c$. If the moments $\langle R^n (R^*)^m \rangle$ converge to a finite limit for $c \rightarrow \infty$, then we can truncate these expansions at terms of $O(1/c)$, whereas if the moments $\langle R^n (R^*)^m \rangle$ diverge, then we need to consider all terms in the series and know all moments of p_R .

From the analytic expressions for the eigenvector moments, presented in the last section, we conclude that the moments of p_R are finite if $\text{var}[K^{\text{out}}] = Bc^\alpha$ ($c \gg 1$) and $\alpha \leq 2$. We explicitly verified that the moments $\langle R^n (R^*)^m \rangle$ ($n+m = 1, 2, 3, 4$) converge to a finite limit if the outdegree distribution $p_{K^{\text{out}}}(k)$ is given by a δ peak (regular graph), a Poisson, or

an exponential distribution, and also the sixth moment of $p_R(r|\lambda)$ converges to a constant in the high connectivity limit for these examples of degree distributions. Thus, we have compelling evidence that all eigenvector moments have a finite limit for $c \rightarrow \infty$ if $\alpha \leq 2$.

For outdegree distributions with $\alpha > 2$, such as the Borel degree distribution, the analysis of Eqs. (S59) and (S60) in the high connectivity limit is more involved because the eigenvector moments scale with c for $c \gg 1$, and therefore we cannot truncate the series at the first terms. Below we illustrate this more clearly by comparing the first few terms of Eq. (S59) for different degree distributions. From now on, we consider, without losing generality, that the eigenvectors are normalized as $\langle |R|^2 \rangle = 1$.

B. High connectivity limit of p_R for $\lambda = \lambda_b \in \mathbb{C}$

Using the results from the previous section and using the notation $F^{(c)}(u, v|\lambda_b) \equiv F(u, v|\lambda_b \in \mathbb{C})$, we can write down the first three nonzero terms of Eq. (S59):

$$F^{(c)}(u, v|\lambda_b) = 1 - \frac{|z|^2}{4c} + \frac{|z|^4 \langle J^4 \rangle \langle |R|^4 \rangle}{64 \langle J^2 \rangle^2 c^2}, \quad (\text{S61})$$

where we substituted $|\lambda|^2 = c \langle J^2 \rangle$.

To proceed further, we need to understand how $\langle |R|^4 \rangle$ behaves for large c . From Eq. (S45), it follows that $\lim_{c \rightarrow \infty} \langle |R|^4 \rangle$ attains a finite value if the variance of $p_{K^{\text{out}}}(k)$ scales as $\text{var}[K^{\text{out}}] \propto c^\alpha$ with $\alpha \leq 2$. In particular, substituting the results for the outdegree distributions of the first section in Eq. (S45), we obtain the asymptotic behaviours:

$$\begin{aligned} \text{Poisson and regular} : \lim_{c \rightarrow \infty} \langle |R|^4 \rangle &= 2, \\ \text{Exponential} : \lim_{c \rightarrow \infty} \langle |R|^4 \rangle &= 4, \\ \text{Borel} : \lim_{c \rightarrow \infty} \frac{\langle |R|^4 \rangle}{c} &= 2. \end{aligned}$$

Hence, for regular, Poisson, and exponential random graphs, for which $\alpha \leq 2$, we can truncate Eq. (S59) at the term of order $O(1/c)$, since the contribution involving $\langle |R|^4 \rangle$ is of the order $O(1/c^2)$. We have also verified that the next term depending on $\langle |R|^6 \rangle$ in Eq. (S59) is of order $O(1/c^3)$ for random graphs with $\alpha \leq 2$. Therefore, for graph ensembles characterized by $\alpha \leq 2$, we set for $c \gg 1$

$$F^{(c)}(u, v|\lambda_b) = 1 - \frac{|z|^2}{4c}. \quad (\text{S62})$$

In the case of the Borel degree distribution, for which $\alpha > 2$, a more refined analysis of Eq. (S59) is needed since the term depending on $\langle |R|^4 \rangle$ in Eq. (S61) is also of the order $O(1/c)$. Therefore, we cannot truncate the series at the second term. We leave the analysis of the high connectivity limit of p_R for graph ensembles with $\alpha > 2$ for a future work.

Substituting Eq. (S62) in Eq. (S56) and expanding the logarithm for $c \gg 1$, we obtain an expression for $g_R^{(c)}(u, v|\lambda_b) \equiv g_R(u, v|\lambda_b \in \mathbb{C})$

$$g_R^{(c)}(u, v|\lambda_b) = \sum_{k=0}^{\infty} p_{K^{\text{out}}}(k) \exp \left[-\frac{k|z|^2}{4c} \right]. \quad (\text{S63})$$

The above equation depends only on the degree distribution and is independent of p_J . Consequently, at this point we have to specify $p_{K^{\text{out}}}(k)$ in order to explicitly perform the summation over the degrees. For regular, Poisson and exponential outdegree distributions (see Eqs. (S2), (S5) and (S10)), we explicitly sum the series and take the limit $c \rightarrow \infty$, obtaining

$$g_R^{(c)}(u, v|\lambda_b) = \exp \left(-\frac{|z|^2}{4} \right) \quad (\text{S64})$$

for Poissonian and regular degree distributions, and

$$g_R^{(c)}(u, v|\lambda_b) = \left(1 + \frac{|z|^2}{4} \right)^{-1} \quad (\text{S65})$$

for exponential degree distributions.

Lastly, we insert Eq. (S64) in Eq. (S55) and calculate the Gaussian integral over u and v to obtain the expression

$$p_R^{(c)}(r|\lambda_b) = \frac{1}{\pi} e^{-|r|^2}, \quad (\text{S66})$$

valid for degree distributions with $\alpha < 2$. The above equations is the Eq. (22) in the main text. The above result is consistent with the standard prediction of random matrix theory according to which the eigenvector components of fully-connected random graphs with Gaussian distributed edges are Gaussian distributed random variables [14]. From Eq. (S66), it is straightforward to derive the so-called Porter-Thomas distribution for the eigenvector amplitudes $\{|R_i|^2\}_{i=1, \dots, N}$ [14]. Although it is natural to expect that the spectral properties of random graphs converge to those of Gaussian random matrices in the limit $c \rightarrow \infty$, Eq. (S63) makes clear that the high connectivity limit of $p_R(r|\lambda_b)$ depends on the degree distribution.

As an example of graph ensemble for which the high connectivity limit of p_R does not converge to the Porter-Thomas distribution of random matrix theory, we compute p_R for an exponential degree distribution ($\alpha = 2$). Substituting Eq.(S65) in Eq. (S55), we obtain

$$p_R^{(c)}(r|\lambda_b) = 4 \int_{-\infty}^{\infty} \frac{du dv}{4\pi^2} e^{iu\text{Re}(r)+iv\text{Im}(r)} \frac{1}{4+u^2+v^2}. \quad (\text{S67})$$

After changing the integration variables in Eq. (S67) to polar coordinates (ρ, θ) , i.e., $u = \rho \cos \theta$ and $v = \rho \sin \theta$, we can integrate over θ and find

$$p_R^{(c)}(r|\lambda_b) = \frac{2}{\pi} \int_0^{\infty} d\rho \frac{\rho}{(4+\rho^2)} J_0(\rho|r|), \quad (\text{S68})$$

where $J_0(x)$ is a Bessel function of the first kind. The integral over ρ is calculated through an integration by parts, leading to the final result

$$p_R^{(c)}(r|\lambda_b) = \frac{2}{\pi} K_0(2|r|), \quad (\text{S69})$$

where $K_0^{\text{out}}(x)$ is a modified Bessel function of the second kind [15]. The above equation is Eq. (24) in the main text.

C. High connectivity limit of p_R for $\lambda = \lambda_b \in \mathbb{R}$

Substituting $\lambda = \pm \sqrt{c\langle J^2 \rangle}$ in Eq. (S60), we obtain the following expression for $F^{(r)}(u|\lambda_b) \equiv F(u|\lambda_b \in \mathbb{R})$ when $c \gg 1$

$$F^{(r)}(u|\lambda_b) = 1 - \frac{u^2}{2c}, \quad (\text{S70})$$

provided $p_{K^{\text{out}}}(k)$ is such that $\alpha \leq 2$. Inserting Eq. (S70) in Eq. (S56) and expanding the logarithm for large c , we find

$$g_R^{(r)}(u|\lambda_b) = \sum_{k=0}^{\infty} p_{K^{\text{out}}}(k) \exp \left[-\frac{ku^2}{2c} \right], \quad (\text{S71})$$

where we introduced the notation $g_R^{(r)}(u|\lambda_b) \equiv g_R(u|\lambda_b \in \mathbb{R})$. If $p_{K^{\text{out}}}(k)$ is a Poisson or regular distribution (or more generally $\alpha < 2$), then

$$g_R^{(r)}(u|\lambda_b) = \exp \left(-\frac{u^2}{2} \right), \quad (\text{S72})$$

while for the exponential degree distribution with $\alpha = 2$ we obtain

$$g_R^{(r)}(u|\lambda_b) = \left(1 + \frac{u^2}{2} \right)^{-1}. \quad (\text{S73})$$

Lastly, we calculate the integral in Eq. (S55). Substituting Eq. (S72) in Eq. (S55) and calculating the Gaussian integrals over u and v , we obtain the following result for $p_R^{(r)}(r|\lambda_b) = p_R^{(r)}(r|\lambda_b \in \mathbb{R})$

$$p_R^{(r)}(r|\lambda_b) = \delta[\text{Im}(r)] \frac{1}{\sqrt{2\pi}} e^{-\frac{1}{2}[\text{Re}(r)]^2}, \quad (\text{S74})$$

valid for $\alpha < 2$. Now we turn our attention to the exponential degree distribution for which $\alpha = 2$. Substituting Eq. (S73) in Eq. (S55), we get

$$p_R^{(r)}(r|\lambda_b) = 2\delta[\text{Im}(r)] \int_{-\infty}^{\infty} \frac{du}{2\pi} e^{iu\text{Re}(r)} \frac{1}{2+u^2}, \quad (\text{S75})$$

which leads to the exponential distribution

$$p_R^{(r)}(r|\lambda_b) = \frac{1}{\sqrt{2}} \delta[\text{Im}(r)] e^{-\sqrt{2}|\text{Re}(r)|}. \quad (\text{S76})$$

D. High connectivity limit of p_R for $\lambda = \lambda_{\text{isol}}$

We set $\lambda = \lambda_{\text{isol}} = c\langle J \rangle$ in Eq. (S60) and truncate the series at the second term, yielding

$$F(u|\lambda_{\text{isol}}) = 1 - \frac{iu\langle R \rangle}{c}. \quad (\text{S77})$$

Analogous to the case $\lambda = \lambda_b$, the moments $\langle R^n \rangle$ ($n = 1, 2, 3, \dots$) of the eigenvector distribution attain a finite value in the limit $c \rightarrow \infty$ if $\alpha \leq 2$ and $\lambda = \lambda_{\text{isol}}$. This ensures that we can truncate the series in Eq. (S60) at the second term. Substituting Eq. (S47) in Eq. (S77) and setting the normalization $\langle R^2 \rangle = 1$, we obtain

$$F(u|\lambda_{\text{isol}}) = 1 - \frac{iu}{\sqrt{\langle K^{\text{out}}(K^{\text{out}} - 1) \rangle}}, \quad (\text{S78})$$

which leads to the following expression for the characteristic function

$$g_R(u|\lambda_{\text{isol}}) = \sum_{k=0}^{\infty} p_{K^{\text{out}}}(k) \exp \left[-\frac{iuk}{\sqrt{\langle K^{\text{out}}(K^{\text{out}} - 1) \rangle}} \right]. \quad (\text{S79})$$

By substituting the variance $\text{var}[K^{\text{out}}] = Bc^\alpha$ in the above equation, we obtain the Eq. (21) appearing in the main text. For $\alpha < 2$, which includes regular and Poisson degree distributions, Eq. (S79) yields for $c \rightarrow \infty$

$$g_R(u|\lambda_{\text{isol}}) = e^{-iu}, \quad (\text{S80})$$

while, for the exponential degree distribution, Eq. (S79) yields for $c \rightarrow \infty$

$$g_R(u|\lambda_{\text{isol}}) = \frac{\sqrt{2}}{\sqrt{2} + iu}. \quad (\text{S81})$$

Finally, in order to obtain $p_R(r|\lambda_{\text{isol}})$, we substitute Eqs. (S80) and (S81) in Eq. (S55), solve the remainder integrals, and take the limit $c \rightarrow \infty$, obtaining the following result for $\alpha < 2$

$$p_R(r|\lambda_{\text{isol}}) = \delta[\text{Im}(r)] \delta[\text{Re}(r) - 1]. \quad (\text{S82})$$

For the exponential degree distribution with $\alpha = 2$, we get

$$p_R(r|\lambda_{\text{isol}}) = \sqrt{2} \delta[\text{Im}(r)] \Theta[\text{Re}(r)] e^{-\sqrt{2}\text{Re}(r)}, \quad (\text{S83})$$

where $\Theta(\dots)$ denotes the Heaviside step function. Eqs. (S82) and (S83) are, respectively, the Eqs. (23) and (25) in the main text, which we aimed to derive. Equations (S69), (S76), (S82), and (S83) explicitly show that the high connectivity limit of the eigenvector distributions at $\lambda = \lambda_{\text{b}}$ and $\lambda = \lambda_{\text{out}}$ is generally not given by the predictions of random matrix theory [14].

S5. COMPARISON WITH DIRECT DIAGONALIZATION RESULTS

We compare the theoretical results for the IPR of $\vec{R}(\lambda_{\text{b}})$ and $\vec{R}(\lambda_{\text{isol}})$, given by Eqs. (9) and (10) in the main text, with results for the IPR obtained from direct diagonalization of adjacency matrices with finite size n .

In order to compare the theory with direct diagonalization, we order the eigenvalues of random matrices \mathbf{A} of size $n \times n$ in the following way:

$$|\lambda_1| \geq |\lambda_2| \geq \dots \geq |\lambda_n|. \quad (\text{S84})$$

If $|\lambda_j| = |\lambda_{j+1}|$, then we order the eigenvalues such that $\text{Im}(\lambda_j) > \text{Im}(\lambda_{j+1})$. Given the above ordering, we define the relative rank of an eigenvalue λ_j as

$$y \equiv \frac{j}{n}. \quad (\text{S85})$$

The eigenvalue outlier λ_{isol} and an eigenvalue λ_{b} located at the boundary of the spectrum both have a relative rank that satisfies $y \rightarrow 0$.

The inverse participation ratio associated with the right eigenvector of λ_j is given by

$$\mathcal{I}(\lambda_j) = \frac{n \sum_{i=1}^n |R_i(\lambda_j)|^4}{(\sum_{i=1}^n |R_i(\lambda_j)|^2)^2}. \quad (\text{S86})$$

In the limit $n \rightarrow \infty$, we consider the function

$$\mathcal{I}_y = \lim_{n \rightarrow \infty} \mathcal{I}(\lambda_{ny}) \quad (\text{S87})$$

defined on the interval $[0, 1]$, which is a deterministic variable if $\mathcal{I}(\lambda_j)$ is self-averaging. For finite n , we are interested in the mean value

$$\langle \mathcal{I}(\lambda_j) \rangle = \left\langle \frac{n \sum_{i=1}^n |R_i(\lambda_j)|^4}{(\sum_{i=1}^n |R_i(\lambda_j)|^2)^2} \right\rangle \quad (\text{S88})$$

and in the distribution $p_{\mathcal{I}(\lambda_j)}$ for the IPR

$$p_{\mathcal{I}(\lambda_j)}(x) = \left\langle \delta(x - \mathcal{I}(\lambda_j)) \right\rangle. \quad (\text{S89})$$

In the first subsection, we present direct diagonalization results for the mean IPR of right eigenvectors, given by Eq. (S88), as a function of the relative rank y , and we show that the theoretical results derived in the main text apply to right eigenvectors with rank $y \approx 0$. In the second subsection, we compute the distribution of the IPR given by Eq. (S89). Finally, in the last subsection, we plot the mean IPR as a function of c for right eigenvectors with small rank $j = 1, 2, 3, 4, 5$ and we compare these results with the Fig. 2 in the main text.

A. IPR as a function of the rank

The properties of $\mathcal{I}(\lambda_j)$ depend whether $\lambda_j \notin \mathbb{R}$ or $\lambda_j \in \mathbb{R}$, since in the former case the right eigenvectors have complex entries, while in the latter case the eigenvectors have real entries. Therefore, it is convenient to consider the conditional averages

$$\langle \mathcal{I}(\lambda_j) | \lambda_j \notin \mathbb{R} \rangle = \left\langle \frac{n \sum_{i=1}^n |R_i(\lambda_j)|^4}{(\sum_{i=1}^n |R_i(\lambda_j)|^2)^2} \middle| \lambda_j \notin \mathbb{R} \right\rangle, \quad (\text{S90})$$

and

$$\langle \mathcal{I}(\lambda_j) | \lambda_j \in \mathbb{R} \rangle = \left\langle \frac{n \sum_{i=1}^n |R_i(\lambda_j)|^4}{(\sum_{i=1}^n |R_i(\lambda_j)|^2)^2} \middle| \lambda_j \in \mathbb{R} \right\rangle. \quad (\text{S91})$$

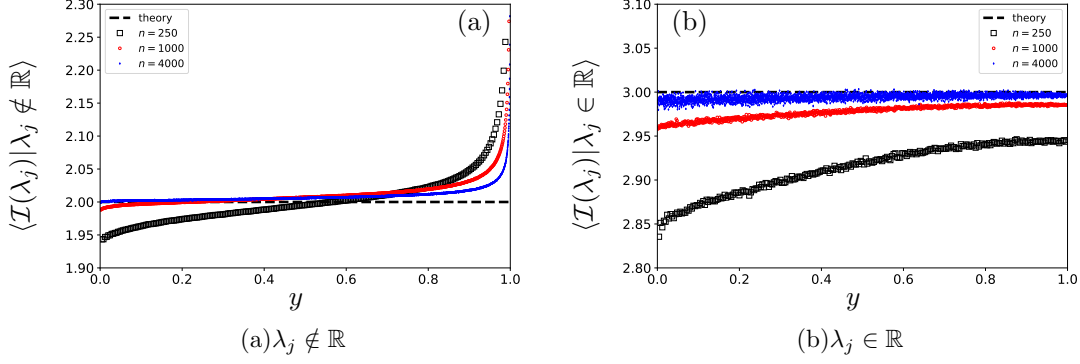


FIG. S2: The average inverse participation ratios $\langle \mathcal{I}(\lambda_j) | \lambda_j \notin \mathbb{R} \rangle$ [Panel (a)] and $\langle \mathcal{I}(\lambda_j) | \lambda_j \in \mathbb{R} \rangle$ [Panel (b)] as a function of $y = j/n$ for a random, regular, and directed graph with $c = 5$ and $p_J(x) = \delta(x - 1)$. Empirical estimates (markers) are compared with the theoretical results (dashed lines) valid for $y \rightarrow 0$ and given by Eq. (S98). Markers for $n = 250$ (black squares) and $n = 1000$ (red circles) are sample means over $1e + 6$ matrix realizations, and markers for $n = 4000$ (blue diamonds) are sample means over $1e + 5$ matrix realizations.

Thus, in the limit $n \rightarrow \infty$, we study the functions

$$\mathcal{I}_y^{(c)} = \lim_{n \rightarrow \infty} \langle \mathcal{I}(\lambda_{ny}) | \lambda_{ny} \notin \mathbb{R} \rangle \quad (\text{S92})$$

and

$$\mathcal{I}_y^{(r)} = \lim_{n \rightarrow \infty} \langle \mathcal{I}(\lambda_{ny}) | \lambda_{ny} \in \mathbb{R} \rangle, \quad (\text{S93})$$

which are defined on the interval $[0, 1]$.

According to the theory presented in the main text, we have that (see Eq. (9))

$$\lim_{y \rightarrow 0} \mathcal{I}_y^{(c)} = \frac{2 [\langle (K^{\text{out}})^2 \rangle - c]}{c(c - \langle J^4 \rangle / \langle J^2 \rangle^2)} \quad (\text{S94})$$

and

$$\lim_{y \rightarrow 0} \mathcal{I}_y^{(r)} = \frac{3 [\langle (K^{\text{out}})^2 \rangle - c]}{c(c - \langle J^4 \rangle / \langle J^2 \rangle^2)}, \quad (\text{S95})$$

provided $\mathcal{I}_y^{(c)}$ and $\mathcal{I}_y^{(r)}$ are self-averaging, and given that $\lambda = \lambda_b$. The quantities $\mathcal{I}_y^{(c)}$ and $\mathcal{I}_y^{(r)}$ are self-averaging if $p_J(x) = \delta(x - 1)$, as discussed in Ref. [13]. If $p_J(x)$ has a finite variance, then Eqs. (S94- S94) apply to a very good approximation, and they are exact if the average values are replaced by the typical values in the right-hand side of Eqs. (S92-S93) [13].

In the special case of the adjacency matrices of directed random graphs such that

$$p_{K^{\text{out}}}(k) = \delta_{k,c} \quad (\text{S96})$$

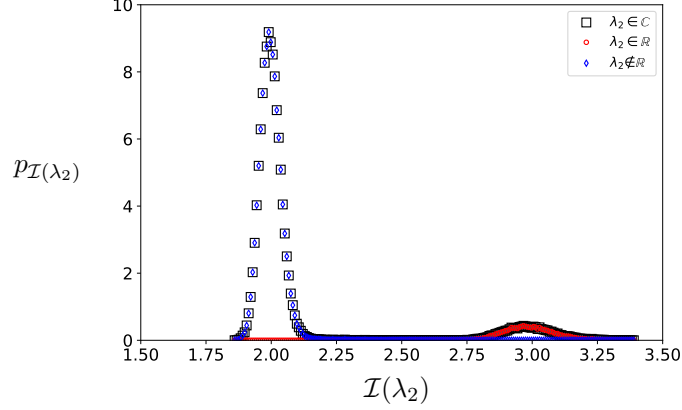


FIG. S3: Distribution $p_{\mathcal{I}(\lambda_2)}$ of $\mathcal{I}(\lambda_2)$ for random, directed, regular graphs with $c = 5$ and $p_J(x) = \delta(x - 1)$ (black squares). The distribution is constructed from $1e + 5$ matrix realizations [same data as in Fig. S2]. We also plot the distribution of $\mathcal{I}(\lambda_2)$ when λ_2 is conditioned to be non-real (red circles) and real (blue diamonds).

and

$$p_J(x) = \delta(J - 1), \quad (\text{S97})$$

we obtain

$$\lim_{y \rightarrow 0} \mathcal{I}^{(c)}(y) = 2, \quad \lim_{y \rightarrow 0} \mathcal{I}^{(r)}(y) = 3, \quad (\text{S98})$$

independent of the average degree c .

In Fig. S2, we estimate $\langle \mathcal{I}(\lambda_{ny}) | \lambda_{ny} \notin \mathbb{R} \rangle$ and $\langle \mathcal{I}(\lambda_{ny}) | \lambda_{ny} \in \mathbb{R} \rangle$ as a function of the relative rank y using sample means obtained from direct diagonalization results of directed random graphs with $p_{K^{\text{out}}}(k) = \delta_{k,c}$, $p_J(x) = \delta(x - 1)$, and $c = 5$, and for three values of the system size: $n = 250, 1000, 4000$. Figure S2 compares the numerical estimates for the mean IPR's at $y \approx 0$ with the theoretical expressions given by Eq. (S98). We observe that Eq. (S98) is well corroborated by the numerical diagonalization results.

In addition, we make a couple of interesting empirical observations. From Fig. 2(b) it is clear that

$$\mathcal{I}^{(r)}(y) = 3 \quad (\text{S99})$$

for any value of $y \in [0, 1]$. On the other hand, from Fig. 2(a) it is not clear what is the value of $\mathcal{I}^{(c)}(y)$ for $y > 0$ [note that the theory for the IPR Eq. (9) only applies at the boundary of the spectrum, i.e. for $y = 0$].

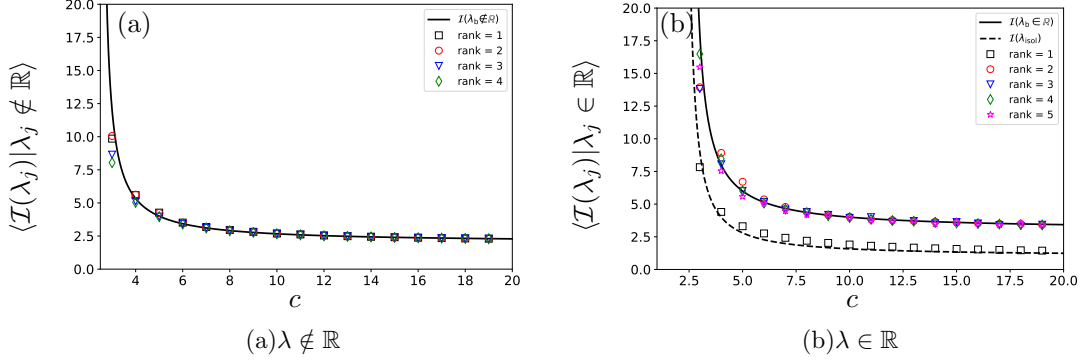


FIG. S4: Sample means for the IPR of right eigenvectors in the adjacency matrices of random directed graphs with $p_{K^{\text{out}}}$ a Poisson distribution of mean c , p_J a Gaussian distribution with mean $\mu = 1$ and variance $\sigma^2 = 1$, and $n = 1000$. Panel (a): each marker is the sample mean over $1e+3$ matrix realizations. The solid line denotes the theoretical value $\mathcal{I}(\lambda_b)$ in Eq. (S103) with $\gamma = 2$. Panel (b): each marker is the sample mean over $1e+4$ matrix realizations. The solid line denotes the theoretical value $\mathcal{I}(\lambda_b)$ in Eq. (S103) with $\gamma = 3$ and the dashed line is the theoretical value $\mathcal{I}(\lambda_{\text{isol}})$ in Eq. (S104). Note that for $c > c_{\text{gap}} = 2$ (see Eq.(4)) the eigenvalue of rank 1 will be the real-valued outlier, and therefore in Panel (a) we have not considered rank 1 eigenvalues.

B. Distribution of the IPR and self-averaging

In Fig. S3, we plot numerical estimates for the distribution of $\mathcal{I}(\lambda_2)$, given by Eq. (S89), for the eigenvalue of rank $j = 2$ of adjacency matrices of directed random graphs with $p_{k^{\text{out}}}(k) = \delta_{k,c}$, $p_J(x) = \delta(x - 1)$, and $c = 5$. We observe that the distribution is peaked around two values, namely, 2 and 3. These two values correspond with $\mathcal{I}(\lambda_2)$ at $\lambda_2 \notin \mathbb{R}$ and $\lambda_2 \in \mathbb{R}$, respectively. This is evident from plotting the distributions conditioned on either $\lambda_2 \notin \mathbb{R}$ or $\lambda_2 \in \mathbb{R}$. These results are consistent with the theoretical values of $\lambda_b \notin \mathbb{R}$ and $\lambda_b \in \mathbb{R}$ in Eq. (S98), and hence corroborate the theory for the IPR of directed random graphs presented in the main paper.

In the limit of large n , the height of the peak centred at the value $\mathcal{I}(\lambda_2) = 3$ will converge to zero for $n \rightarrow \infty$. This is because the number of real eigenvalues of the adjacency matrix of a regular random graph scales as \sqrt{n} , as shown in Figure 3 of Ref. [9]. Moreover, in the limit of large n , the widths of the two peaks in Fig. S3 will converge to zero.

C. Localization transition

Lastly, we show numerical evidence from direct diagonalization results for the localization transition of right eigenvectors in the adjacency matrix of directed random graphs.

In Fig. S4 we present empirical estimates for $\langle \mathcal{I}(\lambda_j) | \lambda_j \notin \mathbb{R} \rangle$ and $\langle \mathcal{I}(\lambda_j) | \lambda_j \in \mathbb{R} \rangle$ for eigenvalues of rank $j = 1, 2, 3, 4, 5$ in random directed graphs with

$$p_{K^{\text{out}}}(k) = \frac{c^k e^{-c}}{k!} \quad (\text{S100})$$

and with

$$p_J(x) = \frac{1}{\sqrt{2\pi\sigma^2}} e^{-\frac{(x-\mu)^2}{2\sigma^2}} \quad (\text{S101})$$

with $\mu = 1$ and $\sigma^2 = 1$. Note that in the limit $n \rightarrow \infty$ graphs with a Poisson outdegree distribution are equivalent to directed Erdős-Rényi graphs for which the C_{ij} are i.i.d. random variables drawn from the distribution

$$p_{C_{ij}}(x) = \frac{c}{n} \delta_{x,1} + \left(1 - \frac{c}{n}\right) \delta_{x,0}. \quad (\text{S102})$$

Fig. S4 should be compared with Fig. 2 in the main text that plots the theoretical expressions in the limit $n \rightarrow \infty$ given by Eqs. (9) and (10). In the present case,

$$\mathcal{I}(\lambda_b) = \frac{(\gamma + 1)c}{c - 5/2} \quad (\text{S103})$$

and

$$\mathcal{I}(\lambda_{\text{isol}}) = \frac{c}{c^3 - 10} \left\{ 3 + (c - 1) \left[5 + c + \frac{16}{c - 2} \right] \right\}. \quad (\text{S104})$$

We observe in Fig. S4 that the theoretical expressions given by Eqs. (S103) and (S104) are very well corroborated by direct diagonalization results. This shows that the theory for the IPR presented in the main text works well even for matrices of relative small size $n = 1000$.

-
- [1] M. E. J. Newman, S. H. Strogatz, and D. J. Watts, Phys. Rev. E **64**, 026118 (2001), URL <https://link.aps.org/doi/10.1103/PhysRevE.64.026118>.
 - [2] B. Bollobás and B. Béla, *Random graphs*, 73 (Cambridge university press, 2001).
 - [3] A. Dembo, A. Montanari, et al., Brazilian Journal of Probability and Statistics **24**, 137 (2010).
 - [4] M. Newman, *Networks: An Introduction* (OUP Oxford, 2010), ISBN 9780199206650, URL <https://books.google.com.br/books?id=q7HVtpYVfC0C>.

- [5] S. N. Dorogovtsev and J. F. Mendes, *Evolution of networks: From biological nets to the Internet and WWW* (OUP Oxford, 2013).
- [6] B. K. Fosdick, D. B. Larremore, J. Nishimura, and J. Ugander, SIAM Review **60**, 315 (2018), <https://doi.org/10.1137/16M1087175>, URL <https://doi.org/10.1137/16M1087175>.
- [7] B. Bollobas, European Journal of Combinatorics **1**, 311 (1980), ISSN 0195-6698, URL <http://www.sciencedirect.com/science/article/pii/S0195669880800308>.
- [8] I. Neri and F. L. Metz, Phys. Rev. Lett. **117**, 224101 (2016).
- [9] F. L. Metz, I. Neri, and T. Rogers, Journal of Physics A: Mathematical and Theoretical **52**, 434003 (2019).
- [10] P. van Mieghem, *Graph Spectra for Complex Networks* (Cambridge University Press, 2012), ISBN 9781107411470, URL <https://books.google.com.br/books?id=hwJFMAEACAAJ>.
- [11] E. Borel, C. R. Acad. Sci. **214**, 452 (1942).
- [12] J. C. Tanner, Biometrika **48**, 222 (1961), ISSN 0006-3444, <https://academic.oup.com/biomet/article-pdf/48/1-2/222/607732/48-1-2-222.pdf>, URL <https://doi.org/10.1093/biomet/48.1-2.222>.
- [13] I. Neri and F. L. Metz, Phys. Rev. Research **2**, 033313 (2020), URL <https://link.aps.org/doi/10.1103/PhysRevResearch.2.033313>.
- [14] A. D. Mirlin, Physics Reports **326**, 259 (2000), ISSN 0370-1573, URL <http://www.sciencedirect.com/science/article/pii/S0370157399000915>.
- [15] I. Gradshteyn and I. Ryzhik, *Table of Integrals, Series, and Products* (Elsevier Science, 2014), ISBN 9781483265643, URL <https://books.google.com.br/books?id=F7jiBQAAQBAJ>.